Chapter 5
MOFs for Pesticide Degradation

Indu Sharma, Kushal Arya, Surinder Kumar Mehta, and Ramesh Kataria

Abstract Despite the perceptible benefits of pesticides, their wide disposal and consumption have been posing a threat to the ecosystem. Several technological advancements have been prompting the utilization of metal–organic frameworks (MOFs) in the field of pesticide degradation. Photochemistry and sonochemistry have been emerging as promising approach toward the degradation of pesticide. Light- and sound-based catalytic degradation of pesticides along with their mechanistic pathways have been listed here. Various parameters affecting photocatalytic degradation have been studied. Ultrasonic waves-based acoustic cavitations assist pesticide degradation by transferring the radicals within the solution. Metal nanoparticles (MNPs), carbon-based materials and metal oxides increase the degradation efficiencies. Herein, various processes having MOF-based materials as a constituent of pesticide degradation have been outlined.

Keywords MOF · Photocatalytic degradation · Pesticides · Sonochemical · Nanoparticles · Light intensity

5.1 Introduction

The booming global population has increased food demands which has indirectly put unrivaled pressure on the agrochemical industries. To accelerate food production, these agro-industries are subjected to involve intense toxic chemicals termed pesticides [1–4]. These are used to put a check over the insects, weeds, fungi and other pests. Moreover, the use of pesticides is also extended up to homes in the guise of sprays and powders for mosquitoes, rats and cockroaches. Pesticides can be broadly categorized as organophosphorus compounds, organochlorine compounds, triazine derivatives, pyrethroids, carbamates, phenoxy acetic acid derivatives, etc. Studies have revealed that only 0.1% of pesticide work on pests while the remaining 99.9%

I. Sharma · K. Arya · S. K. Mehta · R. Kataria (✉)
Department of Chemistry, Centre for Advanced Studies in Chemistry, Panjab University, Chandigarh 160014, India
e-mail: rkataria@pu.ac.in

P. Kumar et al. (eds.), *Metal Organic Framework (MOFs)*,
https://doi.org/10.1007/978-981-97-5971-2_5

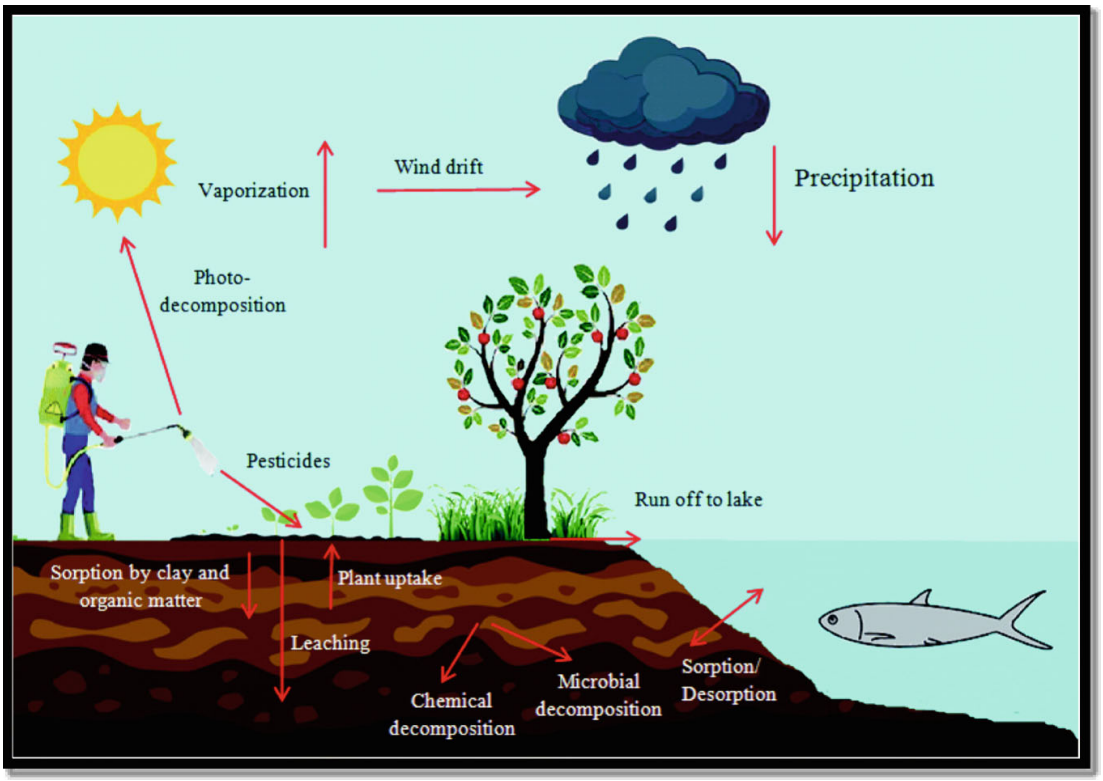

Fig. 5.1 A schematic view of the pesticide cycle in an ecosystem. Adapted from [5]

get sprinkled into the surroundings posing a major threat to human beings and other organisms. Further, among 30 years, there is an increment of 15–20 times in usage of pesticides worldwide. The overview of the cycle of pesticides in our ecosystem is represented in Fig. 5.1.

WHO report says around 3 million people suffer while greater than 200 thousand people die from pesticide poisoning each year [6]. Pesticides along with phenolics, herbicides, dyes, personal care products (PCPs), sulfonates, polycyclic aromatic hydrocarbons (PAHs) and perfluoroalkyl carboxylates are classified as endocrine disruptors (EDs). This is due to the interference of these pollutants with natural hormonal functioning [7, 8]. Pesticides are posing threat to biodiversity by getting into the species in either of three ways [9]:

(1) Dermally—Getting adsorption through the skin.
(2) Breathing—Uptake while inhaling.
(3) Orally—Entry through drinking the toxic water.

Various neurotoxic, genotoxic and cancerous ailments may get developed due to these chemicals. Pesticides are non-biodegradable substances which can create a hazardous effect upon getting mixed with the natural environment. Vector-borne disease, asthma, allergies, influenza and anthrax are prime diseases that may occur to living species upon exposure to these contaminants [10–16] due to organophosphorus pesticides (OPs) aggregation of acetylcholine by inhibiting the activity of acetylcholinesterase. This may lead to various neurological reactions [17, 18]. Among

OPs, diazinon has been considered $C_{12}H_{21}N_2O_3P$ as moderately hazardous class II chemical for living species [19]. It is a highly difficult task to degrade pesticides using conventional methods.

To get a balanced ecological scenario, it an utmost need of hours to eliminate pesticides from the atmosphere. Technologies associated with environmental protection have done vast progressive and innovative efforts to degrade pesticide residue [20]. Many biological as well as chemical methods have been utilized for the decomposition of these hazardous pesticides into non-toxic materials. Biological treatment of pesticides includes either microorganisms as catalysts or enzymes as catalysts. Using microorganisms as catalysts for the degradation process is quite popular. Despite gaining popularity, it is getting faded nowadays due to its poor tolerance to xenobiotics and resistance toward mass transportation of substrate and products [21, 22]. Among enzymes, organophosphorus hydrolase (OPH) is extensively known for the biodegradation of several Ops [23]. Limited stability and inability to reuse and recover are some of the major drawbacks of the enzymatic biodegradation method [24, 25]. Currently, advanced oxidation processes (AOPs) are grabbing the attention in this field due to the involvement of active species [e.g., sulfate radicals ($SO_4^{-}\cdot$) and hydroxyl radicals ($OH\cdot$)]. AOPs avail high recovery, efficacy and stability for degrading organic contaminants [26–30].

5.2 Metal–Organic Frameworks (MOFs) for Pesticide Degradation

A chemist Yaghi 1990 first synthesized a compound named MOF-5 and hence introduced the concept of a metal–organic framework. Metal–organic frameworks (MOFs) are classified as porous hybrid materials where metal centers are linked via multitopic organic linkers. MOFs pertain variety of features such as good binding architecture, large pore volume and surface area. Due to their structural features, there exist diverse applicability of MOFs such as gas storage, sensing, adsorption, separation and microwave absorption [31]. Despite being capable of performing such applicability, MOFs can also be employed as semiconductors such as semiconducting metal oxide. In addition to that, using the linkers, MOFs can absorb photons causing the formation of a charge separation state using a single electron transfer from the excited linker to the metal ion [32, 33] MOFs can be used as a suitable material to degrade pesticides due to their efficacy to act as photocatalysts. In the context of degradation of pesticides, electrolytic, electrocatalytic, sonochemical photocatalytic, photolytic, etc. have been employed till now. MOFs owing to their exceptional and advanced applicability can be used for the above processes. The present chapter describes the involvement of metal–organic frameworks.

Currently, advanced oxidation processes (AOPs) are grabbing the attention in this field due to the involvement of active species [e.g., sulfate radicals ($SO_4^{-}\cdot$) and hydroxyl radicals ($OH\cdot$)]. AOP technologies speed up the degradation and oxidation

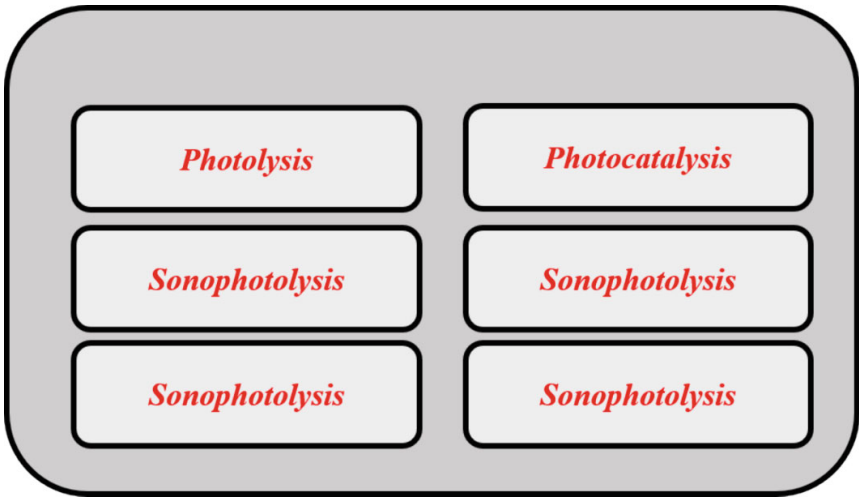

Fig. 5.2 Categorization of various processes involved in light- and ultrasonic wave-based degradation

of a variety of organic as well as inorganic materials that are unresponsive to conventional treatment methods. Until the pesticide moieties are completely transformed to H_2O, CO_2 and mineral acids, AOPs form in situ transitory species, which contribute to the decomposition process. AOPs avail high recovery, efficacy and stability for degrading organic contaminants (Fig. 5.2) [26–28].

(1) **Photolysis**: Exposing a contaminated aqueous solution to UV radiation (UV-A, UV-B, or UV-C) without the use of a catalyst. The organic pollutant molecule is not completely broken down by this process; instead, pollutant molecules are converted into intermediates, some of which may be comparatively more dangerous than the original contaminant molecules.
(2) **Photocatalysis**: The utilization of an anatase-type photocatalyst (ZnO or TiO_2) with exposure to UV radiation.
(3) **Sonolysis:** It is a process of producing hydroxyl radicals in an aqueous environment without the use of a catalyst using ultrasonic irradiation. The disadvantages of this procedure are similar to that of the photolysis.
(4) **Sonocatalysis:** Using a photocatalyst, such as TiO_2, irradiation of ultrasonic waves but not UV irradiation (researchers have found that rutile-type exhibits stronger catalytic efficiency than anatase-type).
(5) **Sonophotolysis:** It is a simultaneous application of ultraviolet light and ultrasonic sound waves without the use of a catalyst of any kind.
(6) **Sonophotocatalysis**: TiO_2 is used as a photocatalyst in sonophotocatalysis, which also uses UV and ultrasonic energy.

Out of these, two major categories are discussed below in the context of pesticide degradation using MOF moieties.

5.3 Photocatalytic Degradation Pathway

The fundamental idea behind photocatalysis is the photoexcitation of a semiconductor caused by electromagnetic radiation that is absorbed under UV/visible light. After absorption of photon energy, the electrons (e^-) in the valence band (VB) are excited to the conduction band (CB), leaving behind the holes (h^+) in VB. As a result, an electron–hole pair will be generated which is responsible for the generation of radical species. Finally, these radicals lead to the degradation of pollutants in non-hazardous components [34]. The photocatalytic approach has various benefits over other conventional wastewater treatment methods including adsorption, membrane filtration, chemical oxidation and microbial degradation. For example, the chemical oxidation method is only economically viable for the removal of contaminants at high concentrations, and biological treatment involves the need for proper pH and temperature control as well as a slow reaction rate. In the case of activated carbon adsorption, the pollutants undergo phase transformation without being broken down, which creates another pollution issue [35, 36]. The photocatalytic degradation method comprises the complete degradation of organic pollutants even in highly low concentrations (in the ppb range) within a small period. Moreover, this process does not produce secondary pollutants, and highly active, inexpensive photocatalysts that can adapt to particularly constructed reactor systems are readily available. Hence, due to its low operating costs and use of light as a green, renewable energy source, photocatalysis has received a great deal of interest over the past few decades [37–39].

5.4 Mechanism of Photocatalytic Degradation Using MOF

In general, five critical phases make up the majority of the photocatalyst-based degradation of organic pollutants: (1) Pollutant molecules adhere to the catalyst's surface; (2) the catalyst absorbs light; (3) a (e^-/h^+) pair forms in the catalyst's CB and VB; (4) superoxide ($^{\bullet}O_2^-$) and hydroxide ($^{\bullet}OH$) radical species are produced; (5) and finally, organic contaminants are oxidized into non-toxic by-products. Photocatalytic action of MOFs can be explained in terms of the HOMO (highest occupied molecular orbital)–LUMO (lowest unoccupied molecular orbital) gap rather than the valence band (VB) and conduction band (CB) theory [40].

LMCT (ligand-to-metal charge transfer) is the most commonly preferred mechanism whereas metal-to-ligand, ligand-to-ligand, metal-to-metal-to-ligand charge transfer mechanisms can also be utilized to describe the mechanism of the photocatalytic degradation of pesticides [41]. In LMCT, organic moieties from MOF help in absorbing light and thereafter generating electrons. Transfer of these photogenerated electrons takes place from HOMO to LUMO of MOFs where it finally reaches up to the surface of the metal-oxo cluster. The LMCT efficiency majorly depends upon $E_{LMCT,}$ i.e., the energy needed for the transfer of electrons from LUMO (linkers) to LUMO (metal nodes) [10]. The E_{LMCT} is about zero or negative for MOFs with

linkers having highly energetic lone pairs and metals of low energy empty orbitals [42, 43]. In the case of Fe-MOFs, the Fe–O cluster can easily produce electrons and holes using photoexcitation. Oxygen molecules form superoxide radicals after capturing the photogenerated electrons [44]. The produced holes on HOMO react with H_2O molecules to give hydroxyl radicals along with the oxidation of organic molecules [45]. Pesticides can be easily degraded by the photogenerated active oxidizing species.

$$\text{Photocatalyst (MOF)} + h\nu \rightarrow h^+(\text{VB}) + e^-(\text{CB}) \tag{5.1}$$

$$H_2O/OH^- + h^+(\text{VB}) \rightarrow OH^{\cdot} + H^+ \tag{5.2}$$

$$O_2 + e^-(\text{CB}) \rightarrow O_2^{-\cdot} \tag{5.3}$$

$$OH^{\cdot}/O_2^{-\cdot} + \text{Pesticides} \rightarrow \text{Degradation products} \tag{5.4}$$

5.5 Influence of Operational Parameters on MOF-Based Degradation of Pesticides

A variety of operational factors that control the photodegradation of various pesticides have a significant impact on the efficiency of the photocatalytic system. The important parameters such as dosage of catalyst, temperature, light intensity, pH, time of light irradiation, initial concentration of pesticides, size, structure and surface area of photocatalyst are responsible for influencing the photocatalytic performance of any catalyst [37, 46, 47] Several scientists have investigated the photodegradation of organic compounds and have concluded that certain conditions are ideal for this process. Numerous studies have discussed the importance of operational parameters (Fig. 5.3).

5.5.1 Effect of Dosage of Photocatalyst (MOF)

The rate of photocatalytic breakdown initially rises with the dosage of photocatalyst and then falls at a higher dosage. Because at an initial stage, there is a higher chance of finding better photoactive sites on the surface of the photocatalyst which leads to an increase in the degradation capacity of the photocatalyst [46]. After a specific threshold of catalyst concentration, a slight decline in rate was seen due to a significant catalyst concentration in an aqueous solution of pesticide can cause the solution to become more turbid, which inhibits the light passage onto the photocatalyst and

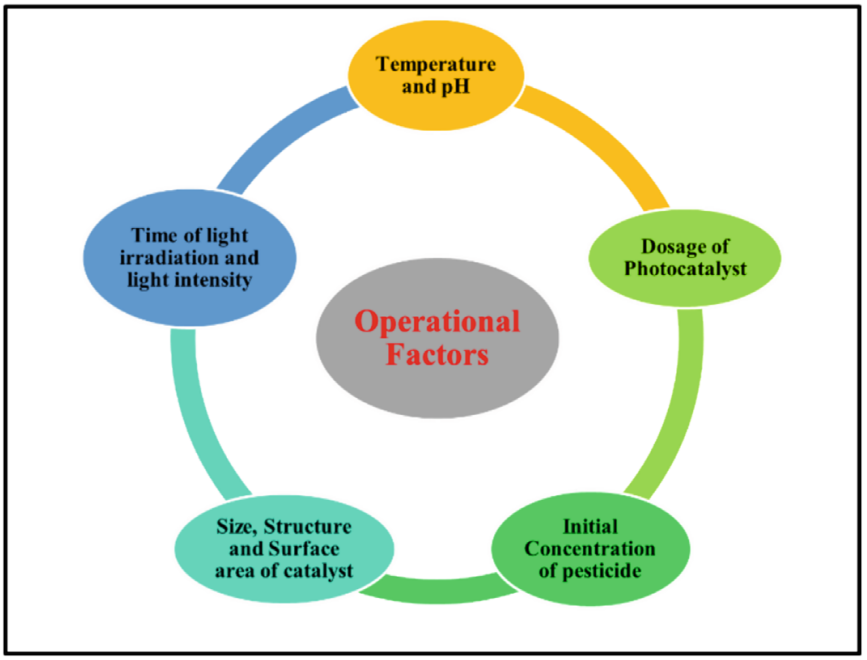

Fig. 5.3 Operating circumstances that affect the photocatalytic degradation process

reduces the production of active radicals. Moreover, the agglomeration of semiconductor particles happens at increasing concentrations, reducing the amount of active surface area that is available for light absorption [34, 37].

Photocatalytic degradation of atrazine over MIL-Co(10) MOF was studied by varying the dosage of MOF from 0.001 to 0.05 g/L. The degradation rate was reached to 83.5% at 0.005 g/L amount of catalyst which was further boosted to 99.9% on increasing the concentration to 0.01 g/L. After that, it remains unchanged on further increasing the dosage of MIL-Co(10) to 0.05 g/L. Hence, the author selected the 0.01 g/L concentration as the optimum dosage for further photodegradation experiments [48]. Similarly, in another work, the amount of photocatalyst (Ce/Eu-HKUST-1 MOF) for light-based degradation of malathion pesticide was fixed as 20 mg which was optimized after performing the degradation experiments by using the different concentrations of MOF ranging from 10 to 30 mg [49].

5.5.2 Effect of Initial Concentration of Pesticides

The adsorption of pesticides onto the surface of the photocatalyst is what makes photocatalysis possible. The pesticide's initial concentration affects how much of it can be absorbed; hence, in a certain photocatalytic reaction, the initial pesticide concentration is a crucial element that must be considered. Only the dye that is

adsorbed on the photocatalyst's surface contributes to the photocatalysis reaction; the dye in the majority of the solution has no impact [46]. According to the literature, the rate of degradation may either reduce or rise as the concentration of the substrate increases [50].

The literature revealed that, at higher starting concentrations of malathion (MA), the degradation rate drops because there are fewer active Ce/Eu-HKUST-1 MOF photocatalytic sites per number of pesticide molecules, indicating that the initial MA concentration has a detrimental impact on the degradation efficiency [49]. On the other hand, the degradation rate of 2-methyl-4-chlorophenoxyacetic acid (MCPA) and 2,4-dichlorophenoxyacetic acid (2,4-D) over Ag-MOF was increased as each pollutant's initial concentration was raised [51].

In general, the rate may initially rise to its highest point before declining. This can be explained by the catalyst's surface reaching saturation in terms of the number of dye molecules and the number of photoactive sites that are available. Because the ability of photocatalysts to generate radicals is reduced at large concentrations; hence, photons of light find it difficult to reach the outer surface of the photocatalyst leading to a decline in the production of photoactive radicals. The effect of the initial concentration of atrazine was studied by varying the initial concentration of the pesticide from 0.5 to 100 mg/L with an optimized dosage of MIL-Co(10) MOF. The obtained results showed the decline in decomposition extent from 100 to 98.5% with an increase in ATZ concentration from 0.5 to 100 mg/L, with a three times reduction in kinetic rate constants. However, almost complete degradation was observed from 1 to 10 mg/L initial concentration of atrazine [48].

5.5.3 Effect of pH and Temperature

When treating wastewater, pH is a critical component that is always taken into account. Adsorption of pollutants onto the semiconductor surface is the first step in photocatalytic degradation. The pH of the system will determine whether the catalyst surface is positively, negatively, or neutrally charged. Hence, surface charges and catalytic reaction potentials could be altered by variations in the solution pH. The point of zero charge (pzc) is used to determine the net charge of the catalyst surface which is defined as the charge at which there are equal numbers of positively and negatively charged particles on the surface. The catalyst surface is protonated and therefore positive for pH values lower than pH_{PZC}, whereas it is deprotonated and consequently negative at pH values higher than $pH_{PZC,}$ or we can say, the catalyst surface is typically positively charged at acidic pH while it is negatively charged at alkaline pH values. In light of this, the charge on the surface of the catalyst is closely associated with the adsorption of pollutant molecules before their light-based catalytic breakdown.

The anionic pesticide molecules such as imidacloprid preferred an acidic pH for adsorption on the surface of the catalyst whereas when the pesticide molecule has cationic nature (chlorpyrifos), the adsorption on the photocatalyst surface is favored

at basic pH. Furthermore, the pH of the solution might influence the reaction among hydroxyl ions and the holes present in the photocatalyst and further affecting the degree of pesticide breakdown. The number of hydrogen ions (H^+) or hydroxide ions (OH^-) in aqueous solutions can have an impact on the protonation or deprotonation of both pesticides and photocatalysts. For example, a decrease in the degradation capacity of BiOBr/UiO-66 toward atrazine pesticide was observed on increasing the initial pH of the solution [52]. More H^+ ions will adhere to the photocatalyst's surface in the acidic environment, making the surface positively charged which is suitable for the adsorption of atrazine due to the presence of highly electronegative chlorine atoms on the surface of the pesticide.

The energy needed for the adsorption as well as the desorption of pesticide molecules is correlated with the influence of temperature on photocatalysts. In the majority of cases, the adsorption is favored by increasing the temperature due to the endocrine nature of the degradation. Moreover, temperature variations also cause materials to undergo phase changes. Adsorption is more likely when the reaction temperature is lower than 80 °C, but an increase in apparent activation energy occurs when the reaction temperature is further lowered below 20 °C. Hence, it has been suggested that a temperature between 20 and 80 °C is ideal for the effective photodegradation of organic pollutants. For example, the 70 °C temperature was optimized for the degradation of 2-methyl-4-chlorophenoxyacetic acid (MCPA) and 2,4-dichlorophenoxyacetic acid (2,4-D) using Ag-MOF [51].

5.5.4 Effect of Size, Structure and Surface Area of MOF

The surface morphology of any MOF catalyst is a major parameter which can affect its degradation efficiency. The size and shape of pores and the surface area of MOFs are important parameters because the surface area of the photocatalyst and organic molecules are directly related. The pace of reaction is controlled by the number of photons striking the photocatalyst, indicating that the degradation only occurs in the absorbed part of the catalyst. Usually, the photodegradation is accelerated by the surface area of the photocatalyst since the materials with high surface areas have more active sites than those with low surface areas. The expansion of surface area has been tried, typically employing very small particles suspended in liquids or formed into a porous film. The surface area of MOFs could be expended via modification of catalyst using external materials like rGO, poly-oxometallates (POMs), nanoparticles and carbon nanotubes (CNTs).

The proper size and shape of pores in any catalyst is a primary requirement to fit the adsorbate molecules for better degradation. The literature revealed that the Zn-MOF-74 is considered an excellent photocatalyst toward glyphosate (GLP) herbicides. This is because it comprises a high surface area (826 $m^2\ g^{-1}$) with a significant micropore volume of 0.344 $cm^3\ g^{-1}$ along with pore width and pore diameter of 1.42 nm and 2.5 nm, respectively [53]. The adsorption capacity of lignin toward methomyl pesticide was increased via the formation of its composite with different

concentration ratios of ZIF-8 MOF [54]. This modification leads to the enhancement of pore size (from 0.11 to 0.55 nm), pore volume (0.01 to 0.41 $cm^3\ g^{-1}$) and surface area (7.22 to 860.5 $dm^2\ g^{-1}$) as well. Based on these results, it was concluded that MOFs are the best catalyst for the adsorption and degradation of pesticides due to their unique surface morphology.

5.5.5 Time of Light Irradiation and Light Intensity

The degradation of pesticides is affected by the intensity of light and the exposure period. The rate of initiation for electron–hole creation in the photochemical process is highly influenced by the intensity of light. It has been demonstrated that a linear increase in the degradation rate occurred at low intensity (below 20 mW/cm^2) because this range of light intensity favored the electron–hole formation rather than their recombination. The degradation rate is independent of this factor at high intensities because the recombination and the electron–hole pair separation compete with one another at this stage.

The exposure time is one of the key factors to govern the degradation potential of any catalyst. More electrons will be excited at the catalyst surface as the contact time increases leading to the enhancement of reactive radical production. The chance of a collision between pesticide molecules and reactive radicals is increased by lengthening the contract period, which may lead to more effective and efficient degradation. The kinetic studies are completely dependent on the agitation time. The change in degradation rate with exposure time determines the suitable kinetic model for obtained experimental results. The kinetic model may be pseudo-first-order, pseudo-second-order or intra-particle based on the time study.

5.6 Metal–Organic Frameworks-Based Photocatalytic Degradation of Pesticides

MOFs can be used as a better substitute for conventional photocatalysts due to their porosity, high tunability and high photocatalytic performance [55–58]. The vast surface area of large adsorption sites for pesticides due to an abundance of large cavities leads to good substrate–catalyst interactions [59]. The degradation efficiency of MOFs depends upon their adsorption efficiency. MOFs can develop a variety of interactions such as van der Waal's, hydrophobic, π–π interactions, electrostatic interactions and hydrogen bonding [60, 61]. All these interactions tend to enhance the link between the MOFs and functional groups of the pesticides. Division of photocatalytic MOFs can be done in three ways:

(1) MOFs in which the secondary building unit, i.e., metal cluster, undergoes photocatalysis,

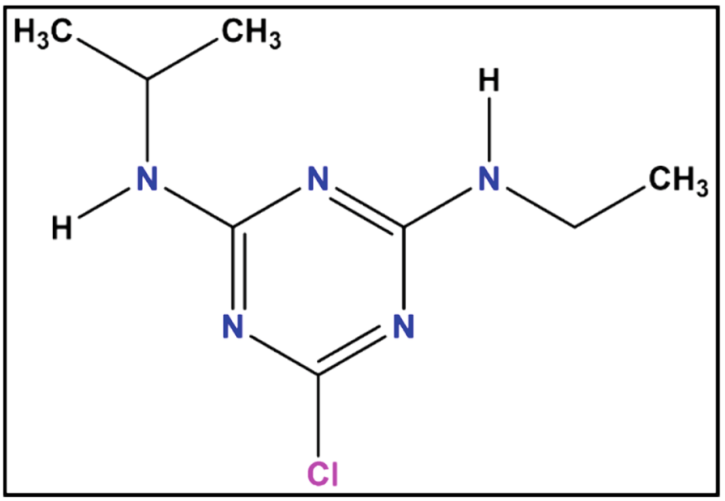

Fig. 5.4 Chemical structure of atrazine

(2) MOFs where certain chromophores, e.g., dye molecules, are used as the organic linkers,
(3) MOFs where certain photoactive species are being inserted inside the cavities of MOFs to initiate photocatalysis.

As the competence of redox pair (e^-/h^+) plays a crucial role while the photocatalytic degradation of pesticides, the composition of MOFs with GO/TiO_2/ZnO/WO_3 with good degradation efficiency is reported [62]. Several MOFs and their composite were found to almost completely degrade malathion including UiO-66@WO_3/GO, UiO-66@ZnO/GO, MIL-53(Fe)/$AgIO_3$ [62, 63] and, similarly, photocatalytic degradation of many pesticides including diazinon, paraquat, bis(p-nitrophenyl)phosphate (BNPP), chlorpyrifos, methyl malathion, nitenpyram (NIT) [64–67]. The degradation mechanism and formation of by-products of some popular pesticides are discussed here (Fig. 5.4).

5.6.1 Atrazine

Atrazine, (2-chloro-4-ethylamino-6-isopropyl-amino-S-triazine) is a herbicide inducing endocrine-disrupting effects. The photocatalytic degradation of atrazine follows pathways such as dealkylation, dichlorination, deamination and denitration followed by C-N bond cleavage [52]. Framework BiOBr/UiO-66 effectively degrade atrazine with up to 88% degradation efficiency. The MOF composite displayed higher efficiency than its bare constituents due to the higher intensity of photocurrent. The separation efficiency of the composite gets enhanced as compared to separate BiOBr and UiO-66 (Fig. 5.5) [52]. Fenton-like degradation of atrazine was achieved by the use of MIL-100(Fe)/ZnO with 80% efficiency. HOMO of MOF (MIL-100(Fe)) produces hydroxyl radical (· OH) using (holes) h^+ following the Fenton-like reaction between Fe(III) of MOF and H_2O_2 to further proceed for the degradation of atrazine [68].

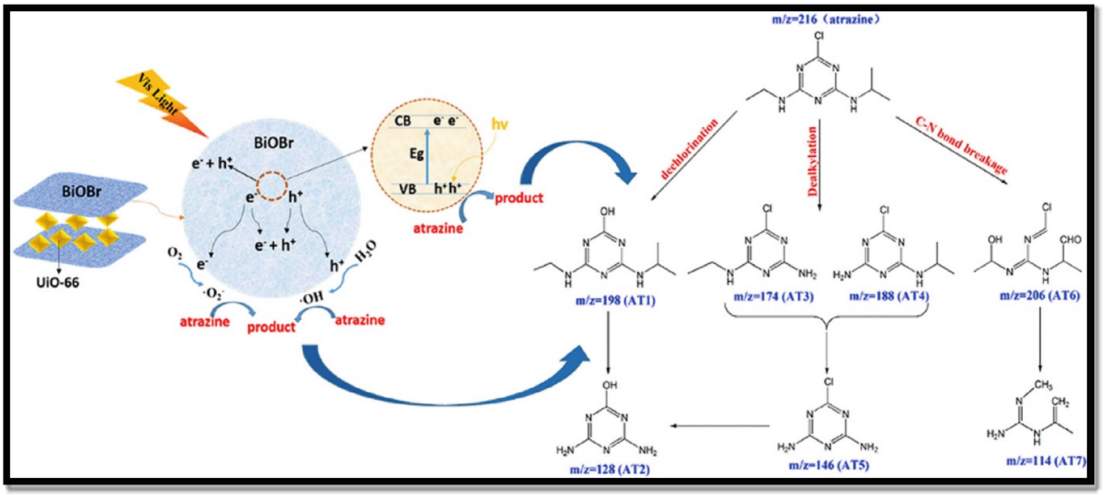

Fig. 5.5 Pictorial representation of photocatalytic degradation mechanism of atrazine over BiOBr/UiO-66. Adapted from [52]

A bimetallic MOF-based heterojunction photocatalyst (MIL-53(Fe/Co)/CeO_2, MIL-CO) was developed for atrazine degradation by visible light-based activation of peroxymonosulfates (PSM) [48]. The 99% decomposition of atrazine was achieved within 60-min exposure to visible light. The dominant radicals in the degradation process were deduced with the help of different radical-trapping scavengers. Numerous intermediates were discovered, and an appropriate degradation pathway was suggested by the author. As depicted in Fig. 5.6, five possible routes [3, 4, 68] for the degradation of ATZ can be in operation, including (i) side chain dealkylation, (ii) oxidation, (iii) hydroxylation, (iv) olefination and (v) dechlorination–hydroxylation.

At initial, PMS molecules are activated to produce huge amounts of SO_4 and OH radicals. These radicals have the propensity to attack the carbon atom that is next to the nitrogen (N) atom through H-abstraction, resulting in the formation of a carbon-centered radical. The SO_4 radicals initiated the oxidation of the pesticide, and the radicals generated through the alkyl side chain can react with O_2 to form peroxide radicals which are further converted into Schiff base. Further hydrolysis and dealkylation of these Schiff base moieties resulted in the formation of various intermediates. At last, these intermediates were subjected to dichlorination, hydroxylation and deamination to produce CO_2, NH_3, Cl_2, H_2O, etc.

5.6.2 Diazinon

Diazinon belongs to a group of pesticides that are somewhat dangerous, along with other chemicals including dichlorodiphenyltrichloroethane (DDT) and chlordane. The World Health Organization (WHO) has designated this class of pesticides as being a member of Group 2A and has classified them as probable carcinogens. Diazinon is less volatile in soil and water, indicating that it will likely remain in water

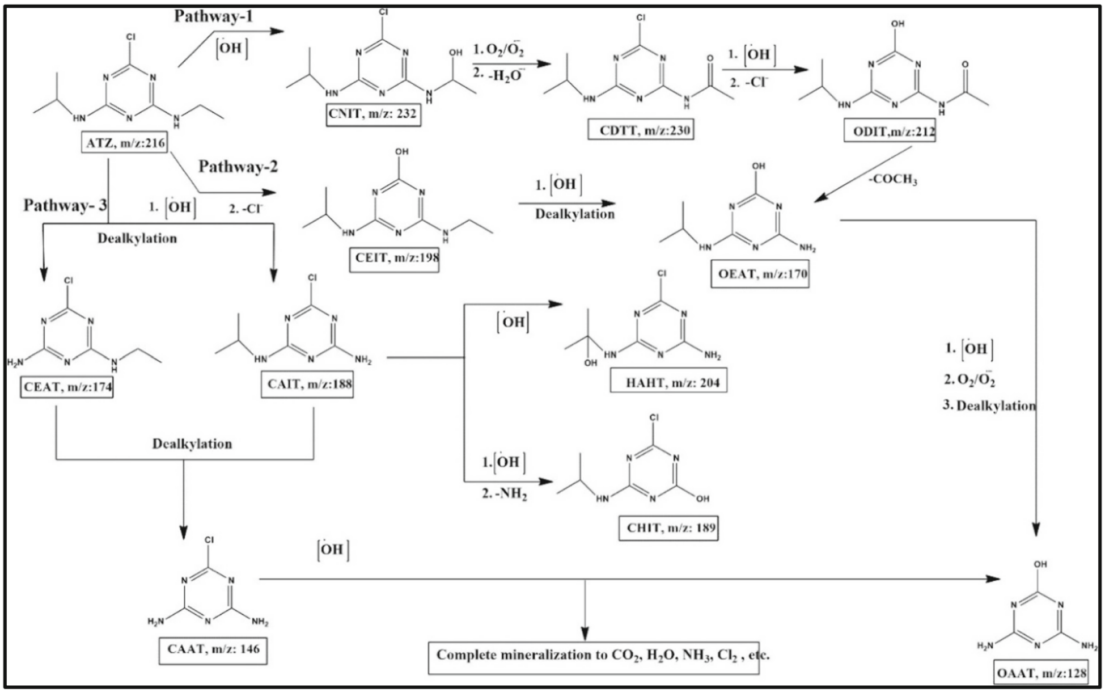

Fig. 5.6 ATZ degradation pathway in the presence of MIL-Co(10)/PMS system. Adapted from [48]

systems. It has been demonstrated that the photocatalytic degradation of diazinon is highly effective and produces less hazardous degradation by-products [69, 70]. MIL-125(Ti), a novel metal–organic framework based on photoactive titanium, has been the subject of recent research efforts for the degradation of diazinon. It exhibits high absorbance ability, good photochemical characteristics and numerous inactive Ti sites which are present throughout this material (Fig. 5.7).

However, because of its activation only in the UV light region and fast charge recombination, which results in poor photocatalytic efficiency, its use in photocatalytic platforms is restricted [71–73]. To overcome this problem, authors designed a composite called MIL-125(Ti)/BP with improved photoactivity where BP stands for

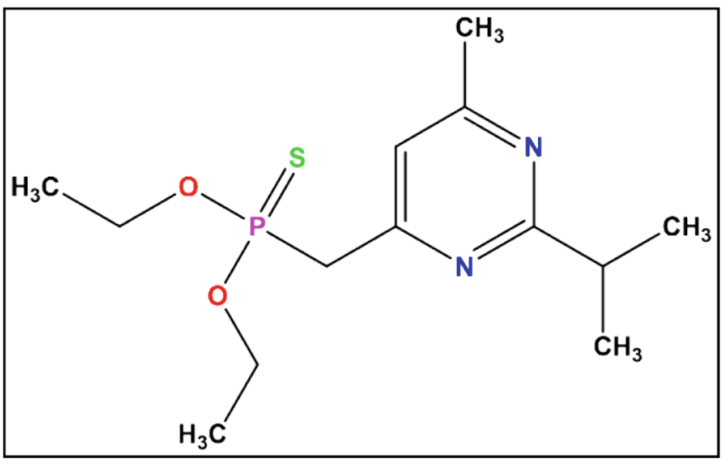

Fig. 5.7 Chemical structure of diazinon

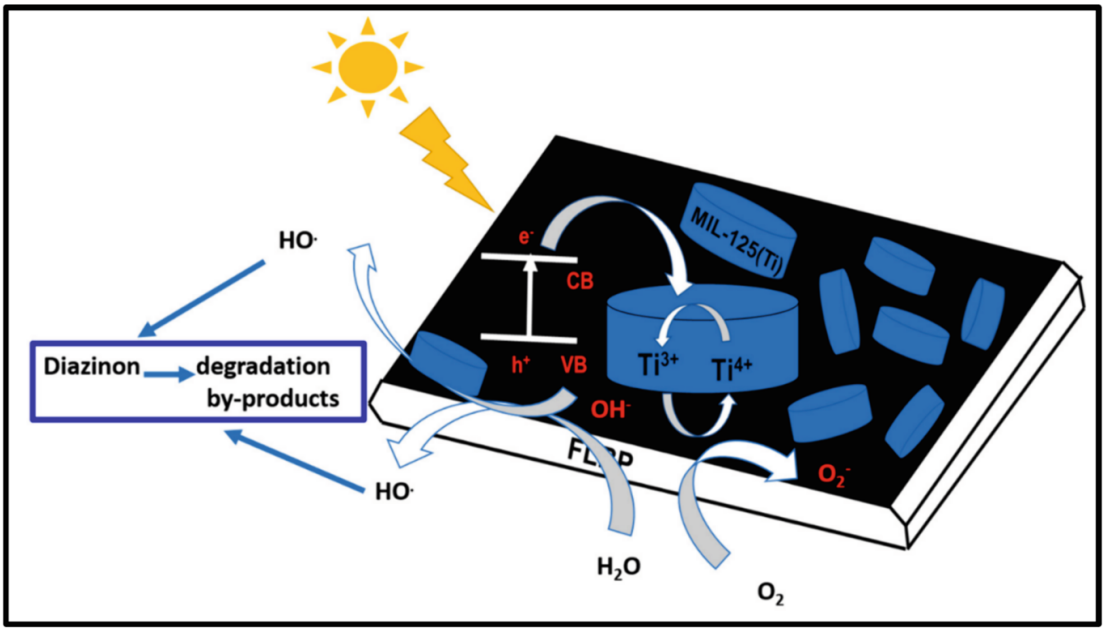

Fig. 5.8 Schematic representation of degradation of diazinon. Adapted from [74]

black phosphorus [74]. It was synthesized by using a two-stage hydrothermal and sonication route. The photodegradation efficiency was improved due to the synergistic interaction between MIL-125(Ti) and BP, as well as the Ti^{3+}-Ti^{4+} intervalence electron transfer as shown in Fig. 5.8.

The 96% removal of diazinon was noticed within 30 min which shows great degradation potential of this MOF toward pesticides.

Another, MOF-based nanocomposite (Fe_3O_4@MOF-2) was also developed for the degradation of the diazinon pesticide [75]. The decomposition pathway and degradation by-products were identified by using GC–MS analysis as shown in Fig. 5.9. The results revealed that the hydroxide and persulfate radicals are principal operational radicals that played a crucial role in this process. Due to their unique structural, catalytic and magnetic characteristics, the Fe_3O_4 particles have been used as a suitable heterogeneous catalyst for the activation of persulfate (Fig. 5.10).

5.6.3 Malathion

An organophosphorus insecticide called malathion is used in a variety of ways to protect human health as well as to grow crops [76] Because it prevents acetylcholinesterase from performing as it should, this pesticide poses a serious risk to the nervous system and malathion poisoning is a cause of disorders such as childhood leukemia, anemia and renal damage [77]. To resolve this issue, a photocatalyst (Ce/Eu-HKUST-1 MOF) was proposed for the sonophotocatalytic degradation of malathion [49]. Based on the radical trapping experiments, h^+ and $^{\cdot}O_2^-$ are considered dominant radicals. The band-gap shrunk and the valence band was moved to

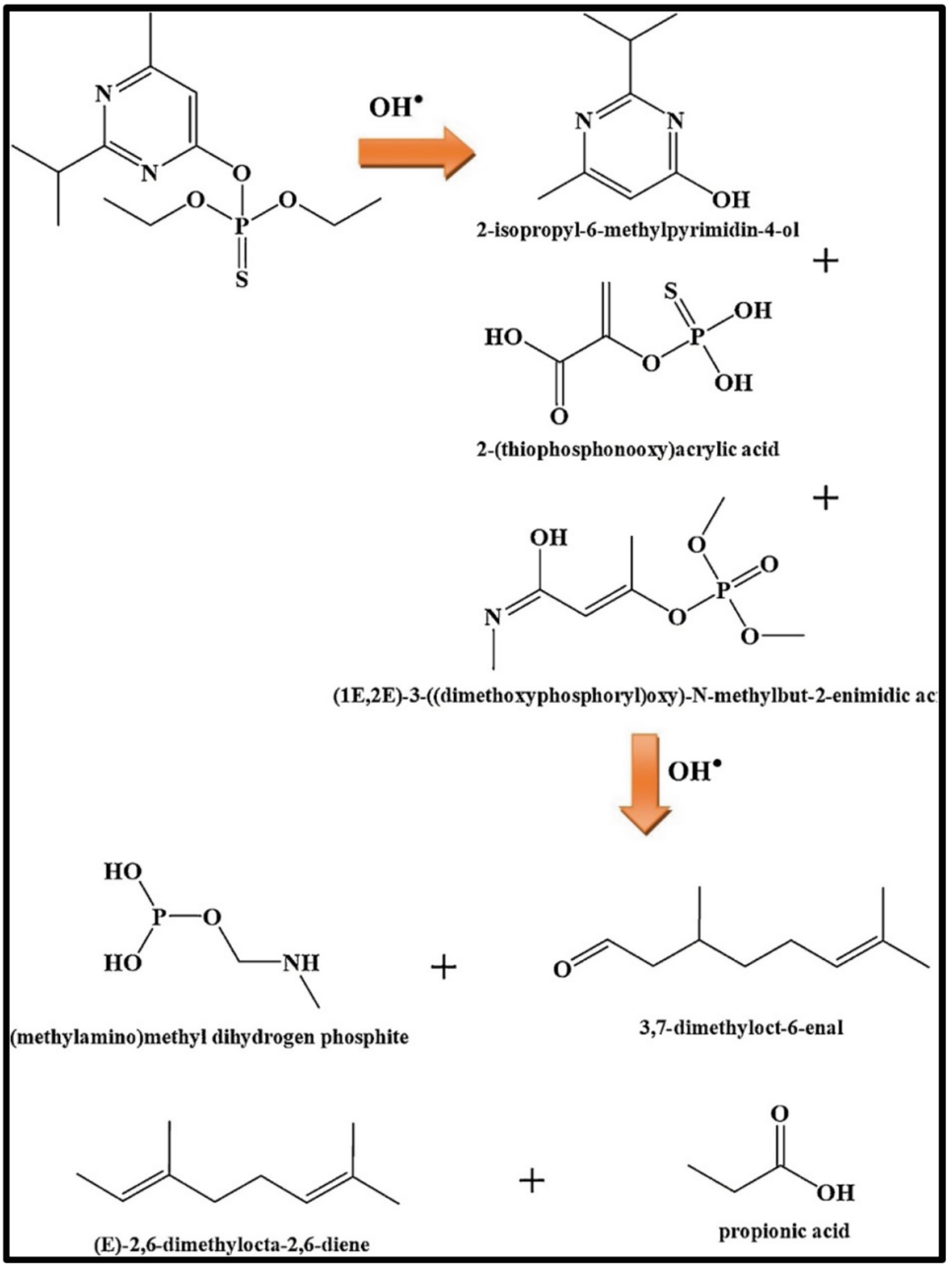

Fig. 5.9 A scheme representing the decomposition pathway of diazinon. Adapted from [75]

the negative phase of potential after the addition of Ce/Eu to HKUST-1. Moreover, the production of $^{\cdot}O_2^-$ radicals also increased in composite material. By using light to create sono-generated carriers, Ce/Eu-HKUST-1 could be stimulated, resulting in the formation of electron–hole pairs in the VBs and CBs as shown in Fig. 5.11. The results showed that, under the ideal conditions of 25 mg/ L malathion, 20 mg dosage of catalyst, 8 (pH) and 25-min agitation time, respectively, the degradation efficiency was 99.99%.

To achieve 100% degradation of malathion, a new ternary nanocomposite UiO-66@WG with high photocatalytic performance was fabricated [62]. After being

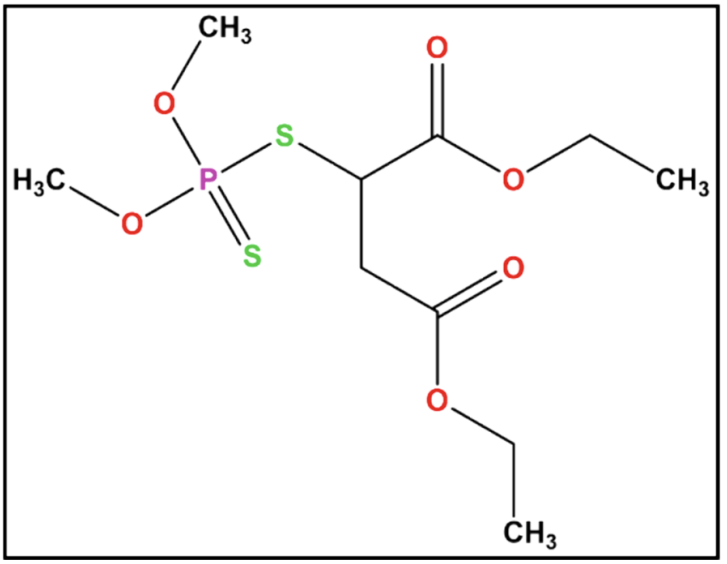

Fig. 5.10 Chemical structure of malathion

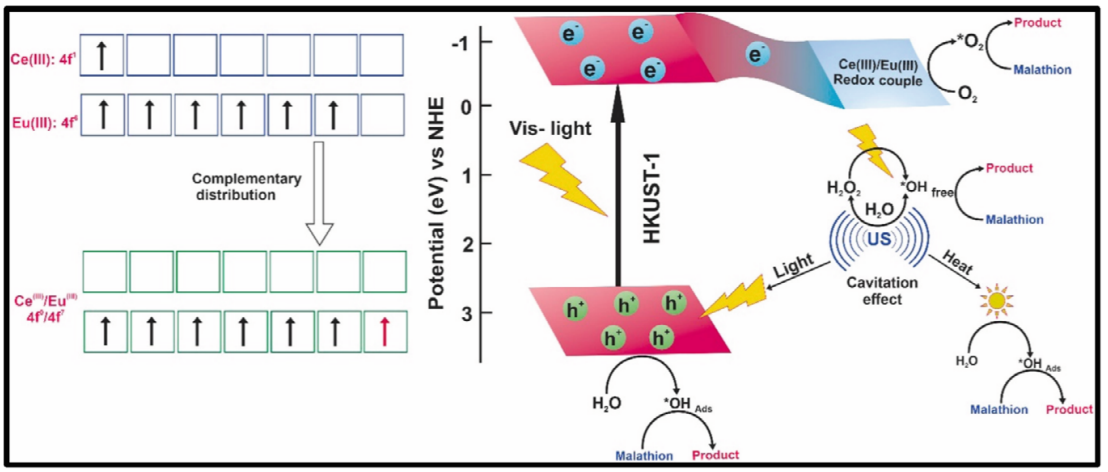

Fig. 5.11 The conceptual illustration of the sonophotodegradation of malathion on the Ce/Eu-HKUST-1 MOF when exposed to the light. Adapted from [49]

exposed to visible light, the excited level of UiO-66 injected electrons into the conduction band of tungsten and h^+ transferred from the valence band of UiO-66 (3.5 eV) to that of W (3.2 eV). The photoexcited electrons and holes can easily generate the $^{\cdot}OH$ and $^{\cdot}O_2^-$ radicals due to the more positive and negative potential of CB concerning the standard E_o values of $^{\cdot}OH/H_2O$ (+2.4 eV) and $O_2/^{\cdot}O_2^-$ (−0.33 eV), respectively, as depicted in Fig. 5.12. Graphene oxide (GO) was used to decrease the electron–hole recombination probability because GO can attract the excited electrons from CB due to its great conjugation and high conductivity. The obtained radical species attack the pesticide (malathion) molecules to decompose the pollutant into non-toxic water and carbon dioxide molecules.

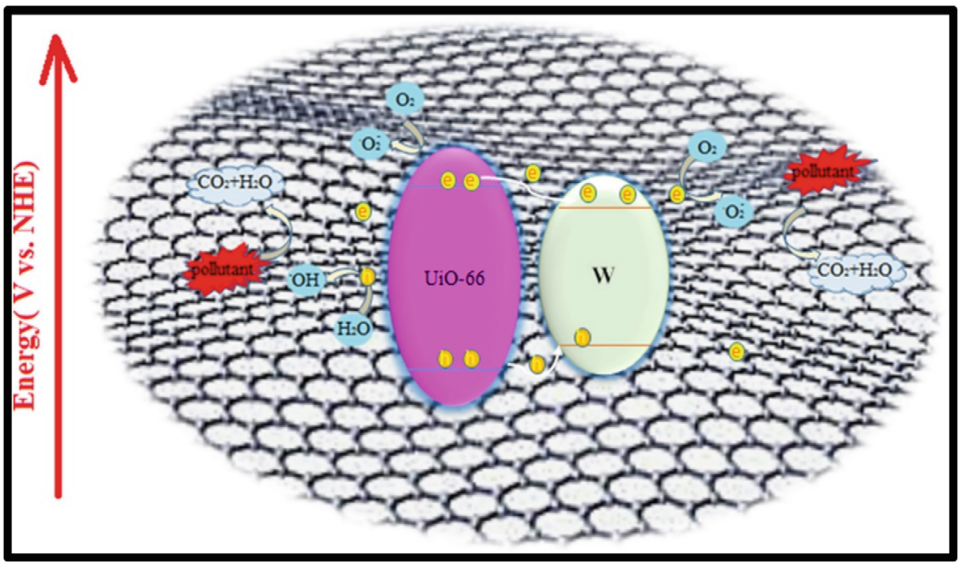

Fig. 5.12 The suggested degradation route of malathion over UiO-66@WG when exposed to visible light. Adapted from [62]

5.6.4 2,4-Dichloro-Phenoxyacetic acid (2,4-D)

2,4-D is a member of the class of herbicides known as phenoxy acids. It is frequently used on broad-leaved weeds including cotton, tobacco and sugarcane in agricultural areas to boost farm output or to control the growth of weeds due to its lower cost and high efficacy [78, 79]. 2,4-D is categorized as a priority contaminant by the US Environmental Protection Agency [80]. According to recent reports, 2,4-D caused genetic harm and cardiac malfunction in zebrafish and can also affect other aquatic species as well as human health [81, 82]. Hence, finding new and effective methods to remove these toxins from aquatic systems is crucial. To eliminate these harmful pollutants from wastewater without creating additional pollutants, MOF-based photocatalysis has been widely employed as an environmentally acceptable technique (Fig. 5.13).

For example, a mesoporous MOF-based photocatalyst named FeCo-MOF was prepared and utilized for degradation of 2,4-D owing to its large surface area, suitable band position for free radical generation, abundant photoactive sites and negligible

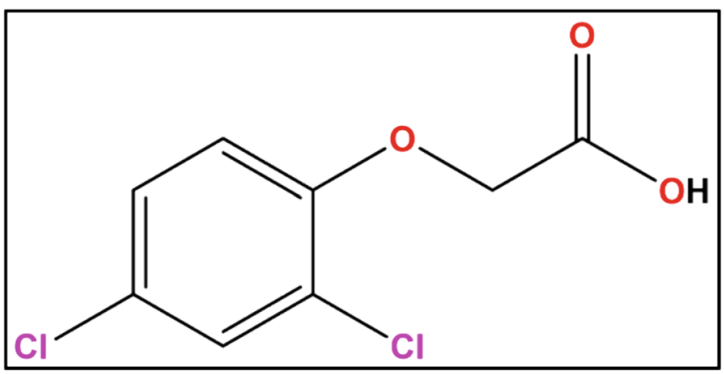

Fig. 5.13 Chemical structure of 2,4-dichlorophenoxyacetic acid

probability of electron–hole recombination [83]. The existence of Fe-μ3-oxo clusters leads to the stimulation of the direct excitation and LMCT pathways whereas the inclusion of cobalt ions in MOF has improved catalytic activity due to their plentiful metal active sites and adjustable porous architectures.

The visible light irradiation to the aqueous solution containing pesticide in the presence of photocatalyst cause the adsorption of photons. After that three different types of excitations can take place: First is direct excitation (direct absorption of light energy by Fe-μ3-oxo clusters); second will be LMCT followed by oxidation of amine group and excitation of metal clusters. In this process, superoxide radicals ($^{\cdot}O_2^-$) played the main role and these are produced by the reaction of photoexcited electrons in CB with O_2 molecules due to more negative conduction band potential energy of FeCo-MOF (−1.28 eV) as compared to the potential needed to generate $^{\cdot}O_2^-$ radicals (−0.28 eV). The calculated degradation percentage was 79.8% within 180 min of light exposure. The expected degradation mechanism is presented in Fig. 5.14.

To increase the degradation rate of 2,4-D to 84%, another MOF-based photocatalyst (UiO-66/g-C_3N_4/Ag) was synthesized [51]. It displayed great reusability and stability over six cycles by using ethanol as a washing solvent. The expected degradation route of 2,4-D is shown in Fig. 5.15. Initially, the excitation of electrons from VB to CB takes place in g-C_3N_4 resulting in the formation of holes in the valence band. The excited e^-s react with oxygen molecules to produce superoxide radicals due to the lower electron potential of CB electrons than the required potential for $^{\cdot}O_2^-$ radical formation. Ag acts as an electron transport bridge to prevent the recombination of electron–hole pairs. The electrons transferred from CB of g-C_3N_4 to CB of UiO-66 react with H_2O_2 to form OH radicals. Further, the harmful pesticide, 2,4-D, undergoes degradation in non-toxic fragments on the influence of these radicals as depicted in the mechanism scheme.

Many more MOF-based photocatalysts were reported in the literature to decompose 2,4-D pollutants with a high degradation rate. For example, a photocatalyst named Ag-MOF can degrade 96% of 2,4-D within 25 min of light irradiation [51]. The high regeneration ability and excellent degradation potential of Ag-MOF toward 2,4-D make it a photocatalyst of great environmental significance for waste water treatment.

5.7 Sonochemical Degradation of Pesticides

Among various AOPs, ultrasound irradiation has been emerging as an effective approach for the degradation of pesticides in water samples. Ultrasound waves have a frequency larger than the realms of human beings, i.e., 20 kHz. The ultrasound waves create acoustic cavitation while traveling through the aqueous medium. Acoustic cavitation is caused by the nucleation, growth and collapsing phenomenon of gas bubbles in liquid [85, 86]. These cavitations may be termed stable and transient cavitation. On higher frequency ranges, the bubbles prefer oscillations rather than

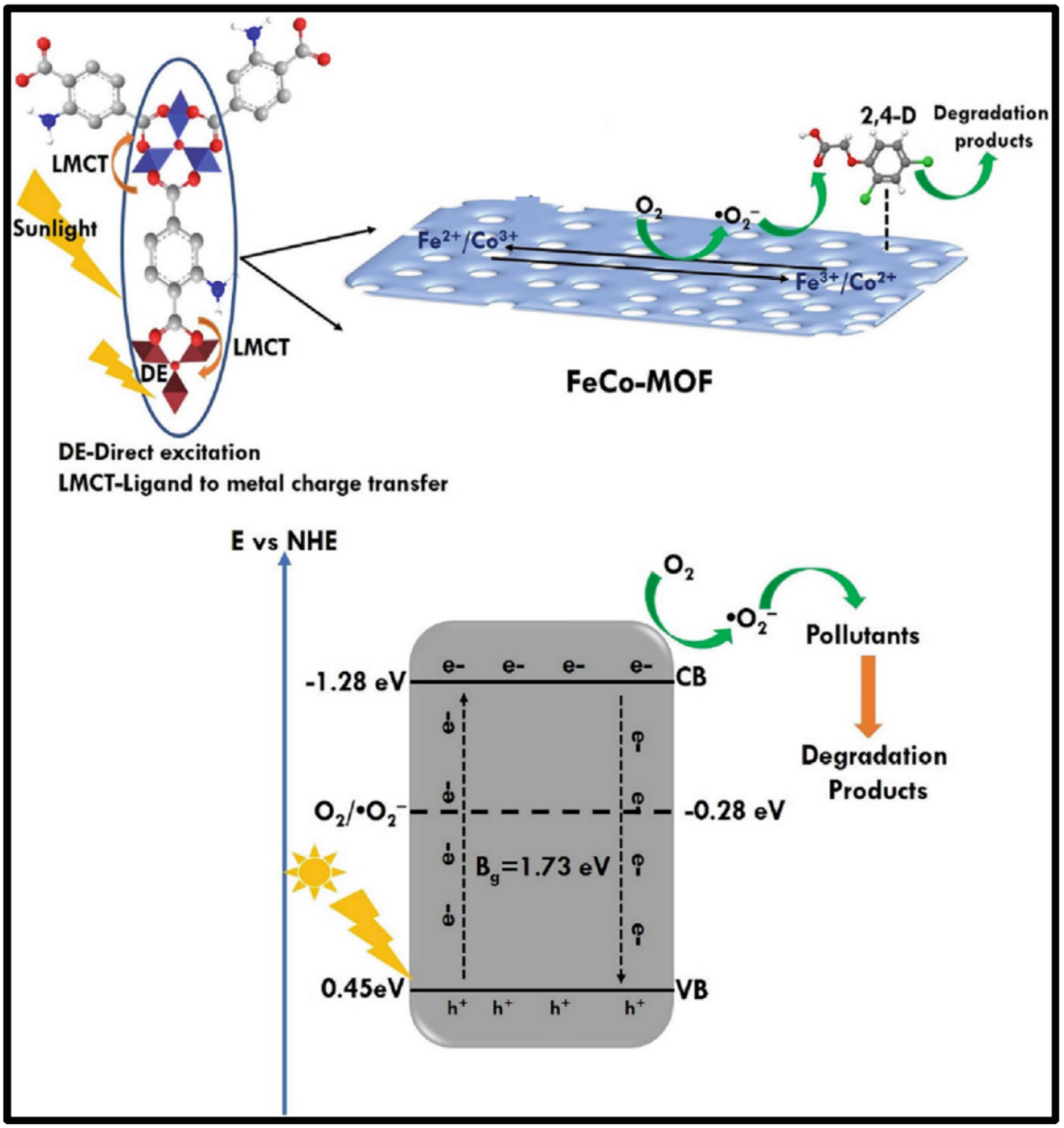

Fig. 5.14 Diagrammatic representation of photocatalytic decomposition mechanism of 2,4-dichloro-phenoxy acetic acid on FeCo-MOF. Adapted from [83]

imploding. This results in stable cavitation. On the other hand, in low-frequency regions, the microbubbles have a life of a few cycles which grow fast for a few cycles and ultimately implode violently [5]. Ultrasound has several advantageous characteristics such as operating at ambient temperature and pressure conditions (Fig. 5.16). Moreover, no pollutant is generated as a by-product during the degradation using the sonochemical method.

Sonophotocatalytic processes involve combining ultrasonic waves, ultrasonic irradiation and semiconductor-based photocatalyst for catalyzing a chemical reaction by producing free radicals in the aqueous solution [87]. This combination provides a synergistic effect to degrade pesticides using highly energetic radicals. Hence, the catalyst can be loaded more because of the consistent and powerful turbulence that

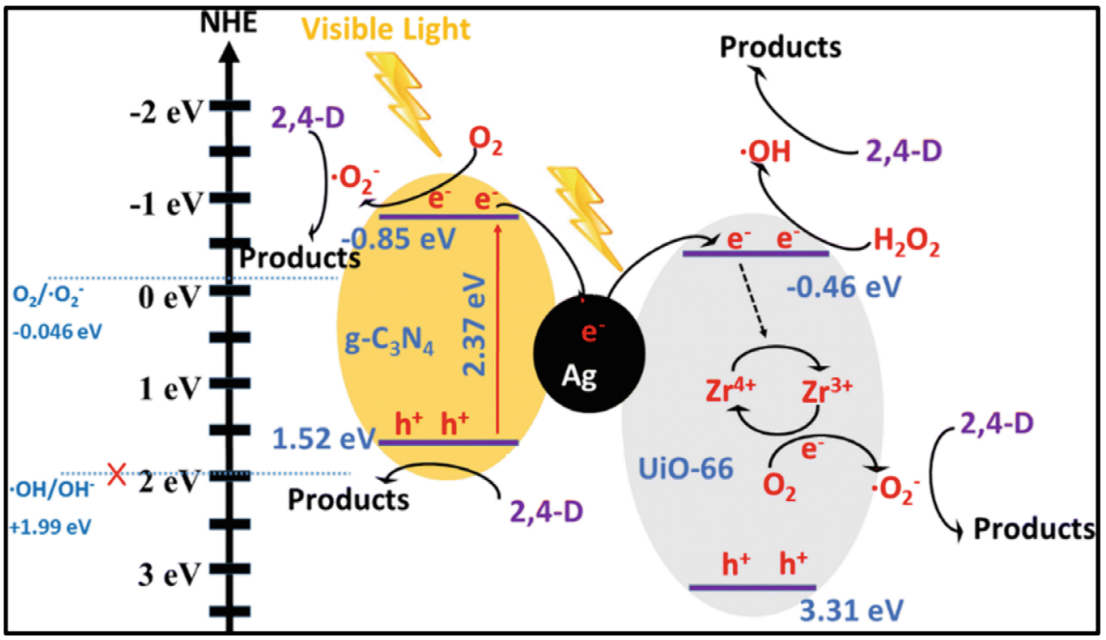

Fig. 5.15 The photocatalytic degradation mechanism of 2,4-D over the photocatalyst UiO-66/g-C_3N_4/Ag under the influence of visible light. Adapted from [84]

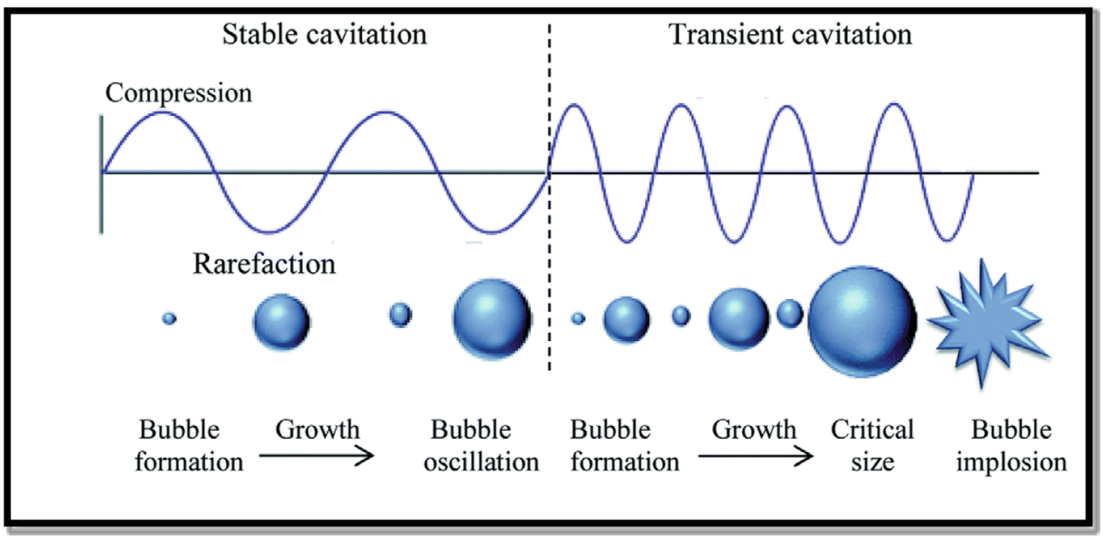

Fig. 5.16 Schematic representation of cavitation bubbles displaying transient and stable cavitation. Adapted from [5]

ultrasound causes. The catalyst slurry's shielding function is removed, as is the barrier to light entering the bulk suspension.

5.8 Mechanism of Sonochemical Degradation Using MOF

In general, two major mechanisms are involved in the sonochemical-based degradation of pesticides depending upon the physiochemical characteristic of the pesticide. The first mechanism is focused on the degradation of more volatile, hydrophobic and apolar compounds. This mechanism is based upon the pyrolysis in the cavitation bubble which is supposed to be the major reaction pathway. The other mechanism involves the degradation or oxidation of pesticides which are less volatile, hydrophilic and polar. This mechanism involves the emergence of hydroxyl radical inside the bubbles which are put away in the bulk liquid and oxidizes the compounds after collapsing [88].

Several MOFs have been reported to show sonochemical degradation of organic pollutants including pesticides. A persulfate-catalyzed nanocomposite (Fe_3O_4@MOF-2) was found to degrade a major pesticide diazinon under an ultrasonic bath of 200–400 WL^{-1}. Almost 100% degradation of diazinon was achieved at pH 3 by using 0.7 gL^{-1} of the nanocomposite [75]. Both the Fe_3O_4 and MOF-2 were acting as semiconductors activated by 'sonoluminescence.' This enhances the photocatalytic process by the generation of hydroxyl radicals. The generation of hydroxyl radicals was as follows:

$$H_2O + \text{Ultrasonic irradiation} \rightarrow OH^{\cdot} + H^{\cdot} \tag{5.5}$$

$$Fe_3O_4@MOF - 2 + \text{Ultrasonic irradiation} \rightarrow h^+ + e^- \tag{5.6}$$

$$H_2O + h^+ \rightarrow OH^{\cdot} + H^+ \tag{5.7}$$

Herein, the photocatalytic role of Fe_3O_4@MOF-2 is further enhanced by ultrasonic irradiation. Several ultrasonic irradiations promoting hydroxyl radical generation in the aqueous solution have been reported in the literature [89, 90].

Abamectin, a slow-acting pesticide which paralyzes the nervous system of insects, has been removed by $Cu_2(OH)PO_4$-HKUST-1 MOF using a sonophotocatalytic process [91]. The instrumentation used for the same is shown below (Fig. 5.17). Coupling of ultrasonic waves with photocatalysis causes the cleavage of oxygen and water molecules. Subsequently, a large number of radicals gets generated which aids the pesticide degradation. The mechanism pathway occurs in the following manner:

$$\text{Photocatalyst} \rightarrow e^- + h^+ \tag{5.8}$$

$$h^+ + \text{Adsorbed } OH^- \rightarrow OH^{\cdot} \tag{5.9}$$

$$e^- + O_2 \rightarrow O_2^{-\cdot} \tag{5.10}$$

$$O_2^{-\cdot} + H_2O \rightarrow HO_2^{\cdot} \tag{5.11}$$

$$O_2^{-\cdot} + HO_2^{\cdot} + H^+ \rightarrow O_2 + H_2O_2 \tag{5.12}$$

$$H_2O + \text{Ultrasonic irradiation} \rightarrow \ OH^{\cdot} + H^{\cdot} \tag{5.13}$$

$$OH^{\cdot} + OH^{\cdot} \rightarrow H_2O_2 \tag{5.14}$$

$$e^- + H^+ + H_2O_2 \rightarrow H_2O + OH^{\cdot} \tag{5.15}$$

$$h^+ + \text{Adsorbed } H_2O \rightarrow H^+ + OH^{\cdot} \tag{5.16}$$

$$h^+ + 2\left(\text{Adsorbed } OH^-\right) \rightarrow OH^- + OH^{\cdot} \tag{5.17}$$

$$OH^{\cdot} + \text{Organic compounds} \rightarrow \text{Intermediates} \tag{5.18}$$

$$OH^{\cdot} + \text{Intermediates} \rightarrow H_2O + CO_2 \tag{5.19}$$

This mechanistic pathway driven by visible light is used in the sonophotocatalytic degradation of abamectin by $Cu_2(OH)PO_4$-HKUST-1 MOF. The degradation percentage (%) for abamectin was measured using the following equation:

$$P(\%) = (1 - C_t/C_0) * 100 \tag{5.20}$$

Further, Ce/Eu functionalized HKUST-1 MOF was also found to degrade malathion effectively using the sonophotodegradation process [49]. Sonophotocatalytic-based oxidation of malathion was carried out in the presence of certain scavengers (benzoquinone (BQ), isopropanol (IPA), ammonium oxalate (AO)) to pull down O_2, OH and hole radicals. After the inclusion of the Ce/Eu redox pair into HKUST-1 MOF, the band gap gets decreased due to the shifting of the valence band (VB) toward the negative potential [92]. Under ultrasound irradiation and visible light, the production of O_2·is improved for the redox pair coupled MOF. Oxidation of holes was done by the adsorbed and oxidized water to form· OH. The ultrasound cavitation creates thermal energy that is consumed to decompose water molecules into OH and H_2O_2. Ultrasonic waves transform H_2O_2 into·OH, and further radicals get generated with the sonocatalyst. Subsequently, the radicals attack the malathion to decompose it [93]. No loss of photocatalytic activity was observed after cyclizing the process.

Apart from MOFs, a variety of other compounds have also been employed in this field for ultrasonic-based degradation. Use of tertiary butyl alcohol, peroxide

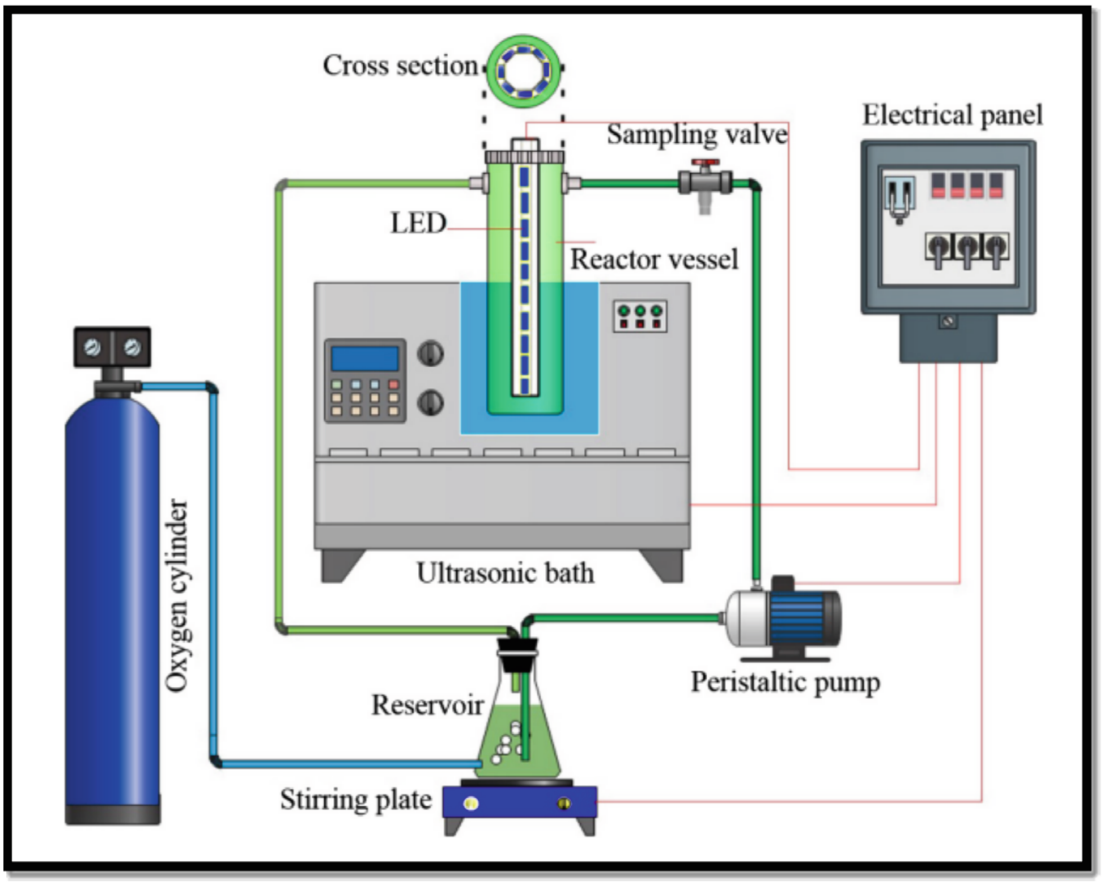

Fig. 5.17 Schematic representation of sonophotocatalytic reactor setup. Adapted from [91]

and certain radical scavengers have been used for the same. 5-methyl benzotriazole (5-MBT) gets readily degraded upon ultrasonic treatment in the aqueous solutions [94]. After the passage of 2 h, nearly complete degradation of 5-MBT took place in the presence of radical scavenger and H_2O_2. The degradation rate majorly declines on the continuous flow due to the reduced substrate concentration. Moreover, the by-products also compete with 5-MBT for the degradation pathways. The proposed mechanism is based on the ·OH substitution on the benzene ring, abstraction of a hydrogen atom by ·OH on the benzylic carbon. Three major reaction pathways have been followed (1) benzylic methyl group oxidation, (2) substitution of hydroxyl radical and (3) ring opening for generation of primary degradation products. Dicofol is an organochlorine pesticide which has endocrine disruptive properties. There exist three fundamental and primary steps involved in the degradation of dicofol under ultrasonic irradiation with the help of tertiary butyl alcohol. Adsorption and diffusion of dicofol to the interface of bubble–liquid is the first step. The second step consists of thermal decomposition with the attack of radicals over the degraded molecule. Finally, intermediates get degraded pyrolytically inside the core of the bubble [95]. DEET (*N*,*N*-dimethyl-m-toluamide) is a residentially used pesticide acting as an insect repellant. Sonochemical degradation of DEET has also been reported in the literature.

5.9 Modified MOF Moieties for Enhanced Degradation Activities

Modification of MOFs helps in the enhancement of their degradation ability. In some cases, the high recombination chances of (e^-/h^+) pairs and the hydrophilic nature of photocatalysts limit the applicability of MOFs in the field of photocatalytic degradation. To overcome these problems, the as-synthesized MOFs could be modified by using different materials like rGO, CNTs, poly-oxometallates and metal or metal oxide nanoparticles. Some examples of modified MOFs and their benefits in degradation are explored below.

5.9.1 Incorporation of Noble Metal Within MOFs

The composition of MOFs with metal offers an advantageous capability for light absorption. The interfacial charge transfers can be made easier, and the rate of recombination of photogenerated electron and hole pairs can be decreased by combining metal and metal–organic frameworks. The variable pore size of metal-incorporated MOF is another significant benefit. As a result, MOF leads to an increase in photocatalytic efficacy in the elimination of numerous organic and chemical contaminants from wastewater. The degradation of the dangerous pesticide 4-ATP (4-aminothiophenol) was accomplished using a copper sheet coated with TiO_2 and cobalt MOF fixed with Ag nanoparticle (Ag/ZIF-67/TiO_2/Cu). Even at low concentrations, the synthesized nanocomposite with Ag encapsulation demonstrated greater surface plasmon resonance than conventionally used substrates. Herein, the total breakdown of 4-ATP was accomplished in 15 min. Additionally, after six cycles of exposure to light, the photocatalytic was unaffected [96].

Phenol is a component of pesticides and dyes and is widely used for household jobs. However, it may irritate the skin, throat and eyes if get exposed. Ag/AgCl/MIL-101(Fe) was synthesized to investigate the role of quinone derivatives in the oxidation of phenol and subsequent reduction of Cr (VI). By consuming a ·OH radical, the phenol ring was opened during phenol oxidation. Singlet oxygen synthesis from $\cdot O_2$ has caused additional quinone derivatives to settle, which accelerates Cr(VI) reduction. This study demonstrates how the silver-based MOF (Ag/AgCl/MIL-101(Fe)) can control the evolution of reactive oxygen species (ROS) and result in considerable phenol photocatalytic degradation [97].

The effectiveness of Ag nanoparticle-incorporated MOF was studied in the breakdown of two phenoxy herbicides named MCPA (2-methyl-4-chlorophenoxyacetic acid) and 2,4-D 2,4-dichlorophenoxyacetic acid The sonochemical irradiation method was used to create the Ag (I) MOF under regulated conditions. To model and optimize the breakdown of herbicides with produced nanocomposite, response surface methods were examined. Herbicides MCPA and 2,4-D degraded at rates of 98% and 96%, respectively (Fig. 5.18) [51].

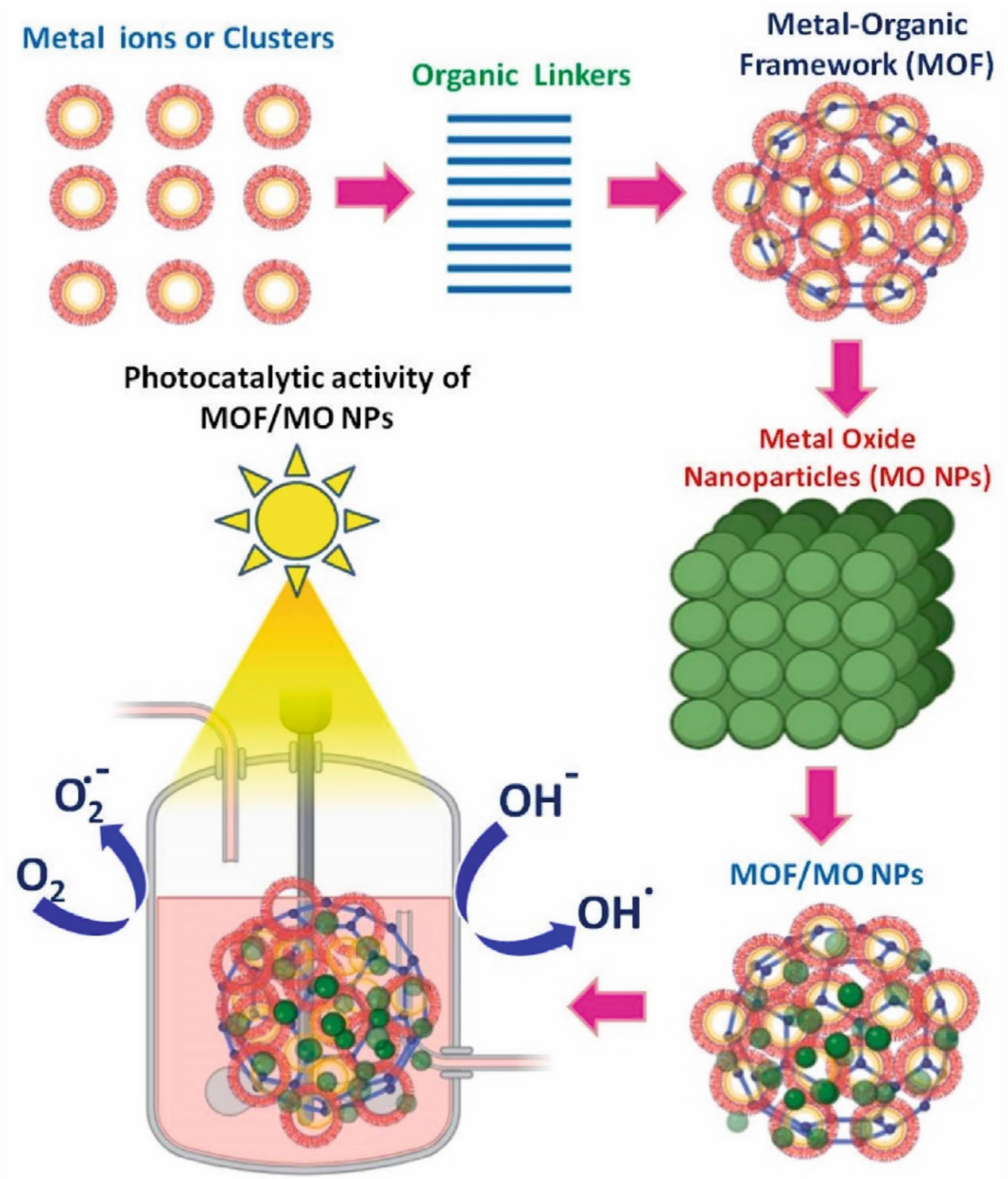

Fig. 5.18 Synthesis and degradation mechanism of MOF/MO NPs. Adapted from [36]

5.9.2 Incorporation of Metal Oxides Within MOFs

Metal oxides are found to effectively enhance the catalytic performance of MOFs. Some metal oxides are vastly used for these applications such as ZnO, TiO_2 and Fe_3O_4. By reducing the size of metal oxide particles at the nanoscale, the photocatalytic activity of metal oxides can further be boosted. Degradation of paraquat has been reported using Cr MOF composite with TiO_2. After the passage of 15 min, the pesticide was degraded up to 88.39%. The catalyst was found very effective even after repetition of up to five cycles [98].

5.9.3 *Incorporation of Graphene-Based Materials*

Carbonaceous catalysts are environmentally friendly, and they are in high demand for wastewater treatment to stop secondary pollution. To activate PMS or PS, carbon-based catalysts such as activated carbon (AC), carbon nanotubes (CNT), reduced graphene oxide (rGO) and nanodiamonds are efficient [99]. The electrical characteristics of carbon would be altered by heteroatom doping, such as N, P, S and B, into carbon frameworks (sp^2-hybridized). Graphene has many characteristics such as flexibility, good electronic conductivity and high surface area. Owing to great adjustments in the electronic properties of graphene, it is widely used nowadays. The sheets of reduced graphene oxide (r-GO) have been extensively used for the degradation processes of organic pollutants. Nanocomposite UiO-66-GO presumably had CBZ (carbendazim) adsorbed on the benzene structure. The organic ligands of the composite were activated by UV radiation and were subsequently able to transfer a photoelectron to the Zr-O clusters. The photoinduced electron in the conduction band subsequently moved fast onto the GO support, significantly improving the separation of carriers and raising the photocatalytic activity (Fig. 5.19). After that, the dissolved oxygen from the system and the photoinduced electron interacted to first create $O_2^{\bullet}$ and subsequently $OH^{\bullet}$. The CBZ molecule was then broken down by the $O_2^{\cdot}$ and $OH^{\cdot}$ radicals during the photolysis into H_2O, CO_2 and other intermediates [100].

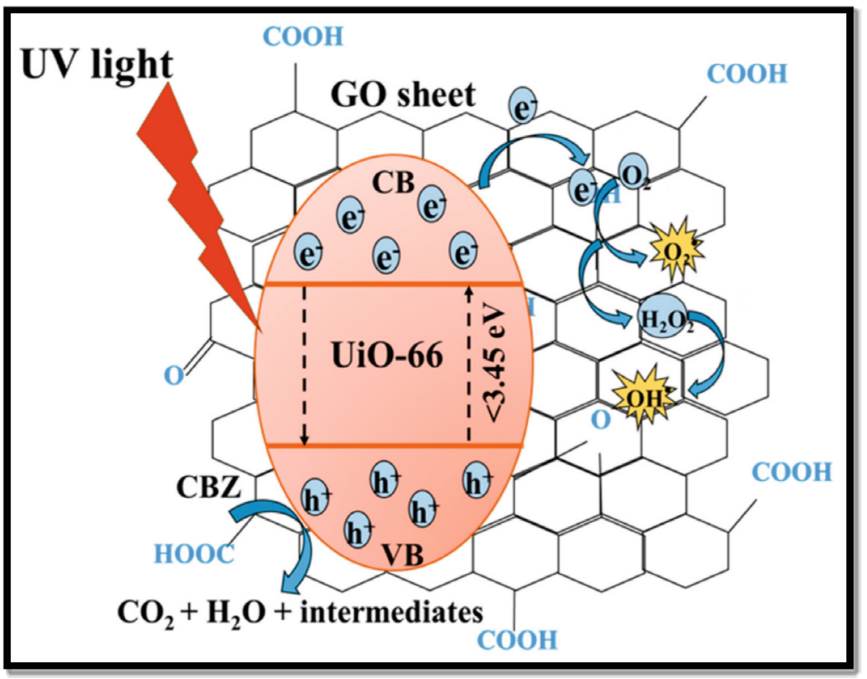

Fig. 5.19 Schematic diagram of a proposed mechanism for photocatalytic oxidation over the UiO-66/GO composite. Adapted from [100]

5.9.4 C_3N_4 Incorporation Within MOFs

Extensive photocatalytic application of carbon nitride has prompted researchers to an increment in the catalytic property. Researchers have become interested in this material because of its remarkable thermal, optical, electrical and chemical properties, ease of synthesis, similar layered structure to that of graphene and photocatalytic performance for solar light [101]. A Co-based MOF (ZIF-67) composite with nanosheets of g-C_3N_4 was synthesized. The prepared nanocomposite displayed excellent photocatalytic degradation of dyes along with 4-chlorophenol. When ZIF-67 was added to g-C_3N_4, the two semiconductors created a heterojunction hybrid that was tightly bound to one another. By leaving the e in the conduction band of g-C_3N_4 under light visible light, the created heterojunction interfaces are thought to enable the migration of photoinduced holes to the ZIF-67, which can be preventing the change of charge recombination and gather free electrons in the conduction band of g-C_3N_4. It aids the catalytic process of the MOF to degrade the above-mentioned organic pollutant [102].

To enhance the stability of MOFs, sometimes inorganic materials (polymers) are incorporated within MOFs. Apart from enhancement in the photocatalytic action of MOFs, polymer incorporation in MOFs proves cost-effective and recyclable. To create MOF-polymer-derived photocatalysts, cerium oxide, zinc dioxide, titanium oxide and some noble metals can be combined with the polymer. The advantages of polymer–MOF systems include recovering catalysts, recycling, nanoparticle release, no particle aggregation and excellent photocatalytic efficiency.

5.10 Conclusion

Over the last few years, extensive studies have promoted researchers to perceive new techniques for the removal of pesticides. A comprehensive study of the light- and sound-based techniques for degrading pesticides is engrooved here. Metal–organic frameworks (MOFs) owing to their catalytic efficiency have been used in photocatalytic and sonophotocatalytic applications. Various parameters affecting the photocatalytic degradation of pesticides have been studied such as pH, temperature, concentration of catalyst and pesticide under both light- and ultrasound-based degradation techniques, and mechanistic pathways of degradation have been explored. Degradation efficiencies of composites of MOFs with r-GO, g-C_3N_4, metal nanoparticles (MNPs), carbon nanotubes (CNTs), etc. were found to get enhanced as compared to bare MOFs. The movement of electrons in conduction bands gets rapid and easier under the support of composites and subsequently enhances the catalytic efficiencies of MOFs. Despite having several degradation pathways, MOFs are still restricted for light- and sound-based catalytic degradation majorly. Hence,

this field can still be explored for this application due to the versatile characteristics of MOFs. Moreover, ultrasound-based techniques are still used only in laboratory environments. Large-scale and industrial approaches for the same can be strived by the researchers.

References

1. Rojas S, Horcajada P (2020) Metal-organic frameworks for the removal of emerging organic contaminants in water. Chem Rev 120:8378–8415. https://doi.org/10.1021/acs.chemrev.9b00797
2. da Silva BF, Jelic A, López-Serna R et al (2011) Occurrence and distribution of pharmaceuticals in surface water, suspended solids and sediments of the Ebro river basin, Spain. Chemosphere 85:1331–1339. https://doi.org/10.1016/j.chemosphere.2011.07.051
3. Cucina M, Tacconi C, Ricci A et al (2018) Evaluation of benefits and risks associated with the agricultural use of organic wastes of pharmaceutical origin. Sci Total Environ 613–614:773–782. https://doi.org/10.1016/j.scitotenv.2017.09.154
4. Casado J, Brigden K, Santillo D, Johnston P (2019) Screening of pesticides and veterinary drugs in small streams in the European Union by liquid chromatography high resolution mass spectrometry. Sci Total Environ 670:1204–1225. https://doi.org/10.1016/j.scitotenv.2019.03.207
5. Pirsaheb M, Moradi N (2020) Sonochemical degradation of pesticides in aqueous solution: Investigation on the influence of operating parameters and degradation pathway-a systematic review. RSC Adv 10:7396–7423. https://doi.org/10.1039/c9ra11025a
6. Islam SMA, Yeasmin S, Islam MS, Islam MS (2017) Binding affinity and adhesion force of organophosphate hydrolase enzyme with soil particles related to the isoelectric point of the enzyme. Ecotoxicol Environ Saf 141:85–92. https://doi.org/10.1016/j.ecoenv.2017.03.010
7. Jun BM, Hwang HS, Heo J et al (2019) Removal of selected endocrine-disrupting compounds using Al-based metal organic framework: Performance and mechanism of competitive adsorption. J Ind Eng Chem 79:345–352. https://doi.org/10.1016/j.jiec.2019.07.009
8. Canle M, Fernández Pérez MI, Santaballa JA (2017) Photocatalyzed degradation/abatement of endocrine disruptors. Curr Opin Green Sustain Chem 6:101–138. https://doi.org/10.1016/j.cogsc.2017.06.008
9. Helfrich LA (2009) Pesticides and Aquatic Animals: A Guide to Reducing Impacts on Aquatic Systems. Virginia Coop Ext 420:1–24
10. Pi Y, Li X, Xia Q et al (2018) Adsorptive and photocatalytic removal of persistent organic pollutants (POPs) in water by metal-organic frameworks (MOFs). Chem Eng J 337:351–371. https://doi.org/10.1016/j.cej.2017.12.092
11. Tkaczyk A, Mitrowska K, Posyniak A (2020) Synthetic organic dyes as contaminants of the aquatic environment and their implications for ecosystems: a review. Sci Total Environ 717:137222. https://doi.org/10.1016/j.scitotenv.2020.137222
12. Kant R (2012) Textile dyeing industry an environmental hazard. Nat Sci 04:22–26. https://doi.org/10.4236/ns.2012.41004
13. Quesada HB, Baptista ATA, Cusioli LF et al (2019) Surface water pollution by pharmaceuticals and an alternative of removal by low-cost adsorbents: a review. Chemosphere 222:766–780. https://doi.org/10.1016/j.chemosphere.2019.02.009
14. Lacorte S, Luis S, Gómez-Canela C et al (2018) Pharmaceuticals released from senior residences: occurrence and risk evaluation. Environ Sci Pollut Res 25:6095–6106. https://doi.org/10.1007/s11356-017-9755-1
15. Danner MC, Robertson A, Behrends V, Reiss J (2019) Antibiotic pollution in surface fresh waters: occurrence and effects. Sci Total Environ 664:793–804. https://doi.org/10.1016/j.scitotenv.2019.01.406

16. Tijani JO, Fatoba OO, Babajide OO, Petrik LF (2016) Pharmaceuticals, endocrine disruptors, personal care products, nanomaterials and perfluorinated pollutants: a review. Environ Chem Lett 14:27–49. https://doi.org/10.1007/s10311-015-0537-z
17. Luo XJ, Zhao J, Li CX et al (2016) Combinatorial evolution of phosphotriesterase toward a robust malathion degrader by hierarchical iteration mutagenesis. Biotechnol Bioeng 113:2350–2357. https://doi.org/10.1002/bit.26012
18. Blatchford PA, Scott C, French N, Rehm BHA (2012) Immobilization of organophosphohydrolase OpdA from *Agrobacterium radiobacter* by overproduction at the surface of polyester inclusions inside engineered *Escherichia coli*. Biotechnol Bioeng 109:1101–1108. https://doi.org/10.1002/bit.24402
19. Tabasideh S, Maleki A, Shahmoradi B et al (2017) Sonophotocatalytic degradation of diazinon in aqueous solution using iron-doped TiO_2 nanoparticles. Sep Purif Technol 189:186–192. https://doi.org/10.1016/j.seppur.2017.07.065
20. Xia T, Lin Y, Li W, Ju M (2021) Photocatalytic degradation of organic pollutants by MOFs based materials: a review. Chinese Chem Lett 32:2975–2984. https://doi.org/10.1016/j.cclet.2021.02.058
21. Cho CMH, Mulchandani A, Chen W (2002) Bacterial cell surface display of organophosphorus hydrolase for selective screening of improved hydrolysis of organophosphate nerve agents. Appl Environ Microbiol 68:2026–2030. https://doi.org/10.1128/AEM.68.4.2026-2030.2002
22. Singh S, Kang SH, Mulchandani A, Chen W (2008) Bioremediation: environmental clean-up through pathway engineering. Curr Opin Biotechnol 19:437–444. https://doi.org/10.1016/j.copbio.2008.07.012
23. Masson P, Josse D, Lockridge O et al (1998) Enzymes hydrolyzing organophosphates as potential catalytic scavengers against organophosphate poisoning. J Physiol Paris 92:357–362. https://doi.org/10.1016/S0928-4257(99)80005-9
24. Breger JC, Walper SA, Oh E et al (2015) Quantum dot display enhances activity of a phosphotriesterase trimer. Chem Commun 51:6403–6406. https://doi.org/10.1039/c5cc00418g
25. Seo JS, Lee S, Poulter CD (2013) Regioselective covalent immobilization of recombinant antibody-binding proteins A, G, and L for construction of antibody arrays. J Am Chem Soc 135:8973–8980. https://doi.org/10.1021/ja402447g
26. Sharma A, Ahmad J, Flora SJS (2018) Application of advanced oxidation processes and toxicity assessment of transformation products. Environ Res 167:223–233. https://doi.org/10.1016/j.envres.2018.07.010
27. Kanakaraju D, Glass BD, Oelgemöller M (2018) Advanced oxidation process-mediated removal of pharmaceuticals from water: a review. J Environ Manage 219:189–207. https://doi.org/10.1016/j.jenvman.2018.04.103
28. Yang Y, Zeng Z, Zhang C et al (2018) Construction of iodine vacancy-rich BiOI/Ag@AgI Z-scheme heterojunction photocatalysts for visible-light-driven tetracycline degradation: transformation pathways and mechanism insight. Chem Eng J 349:808–821. https://doi.org/10.1016/j.cej.2018.05.093
29. Yang Y, Zhang C, Huang D et al (2019) Boron nitride quantum dots decorated ultrathin porous g-C3N4: Intensified exciton dissociation and charge transfer for promoting visible-light-driven molecular oxygen activation. Appl Catal B Environ 245:87–99. https://doi.org/10.1016/j.apcatb.2018.12.049
30. Zhou C, Lai C, Huang D et al (2018) Highly porous carbon nitride by supramolecular preassembly of monomers for photocatalytic removal of sulfamethazine under visible light driven. Appl Catal B Environ 220:202–210. https://doi.org/10.1016/j.apcatb.2017.08.055
31. Hirscher M, Panella B (2005) Nanostructures with high surface area for hydrogen storage. J Alloys Compd 404–406:399–401. https://doi.org/10.1016/j.jallcom.2004.11.109
32. Pan Y, Liu W, Liu D et al (2019) A 3D metal-organic framework with isophthalic acid linker for photocatalytic properties. Inorg Chem Commun 100:92–96. https://doi.org/10.1016/j.inoche.2018.12.025

33. Bibi R, Huang H, Kalulu M et al (2019) Synthesis of amino-functionalized Ti-MOF Derived yolk-shell and hollow heterostructures for enhanced photocatalytic hydrogen production under visible light. ACS Sustain Chem Eng 7:4868–4877. https://doi.org/10.1021/acssuschemeng.8b05352
34. Arya K, Kumar A, Sharma A et al (2022) A hybrid nanocomposite of coordination polymer and rGO for photocatalytic degradation of safranin-O dye under visible light irradiation. Top Catal 65:1924–1937. https://doi.org/10.1007/s11244-022-01701-7
35. Wen Y, Feng M, Zhang P et al (2021) Metal organic frameworks (MOFs) as photocatalysts for the degradation of agricultural pollutants in water. ACS ES&T Eng 1:804–826. https://doi.org/10.1021/acsestengg.1c00051
36. Ramalingam G, Pachaiappan R, Kumar PS et al (2022) Hybrid metal organic frameworks as an exotic material for the photocatalytic degradation of pollutants present in wastewater: a review. Chemosphere 288:132448. https://doi.org/10.1016/j.chemosphere.2021.132448
37. Bruckmann FS, Schnorr C, Oviedo LR et al (2022) Adsorption and photocatalytic degradation of pesticides into nanocomposites: a review. Molecules 27. https://doi.org/10.3390/molecules27196261
38. Zanoni MVB, Irikura K, Perini JAL et al (2022) Recent achievements in photoelectrocatalytic degradation of pesticides. Curr Opin Electrochem 35:101020. https://doi.org/10.1016/j.coelec.2022.101020
39. Barjasteh-Askari F, Nasseri S, Nabizadeh R et al (2022) Photocatalytic removal of diazinon from aqueous solutions: a quantitative systematic review. Environ Sci Pollut Res 29:26113–26130. https://doi.org/10.1007/s11356-022-18743-9
40. Nasalevich MA, Van Der Veen M, Kapteijn F, Gascon J (2014) Metal-organic frameworks as heterogeneous photocatalysts: advantages and challenges. CrystEngComm 16:4919–4926. https://doi.org/10.1039/c4ce00032c
41. Wen M, Li G, Liu H et al (2019) Metal-organic framework-based nanomaterials for adsorption and photocatalytic degradation of gaseous pollutants: recent progress and challenges. Environ Sci Nano 6:1006–1025. https://doi.org/10.1039/c8en01167b
42. De Vos A, Hendrickx K, Van Der Voort P et al (2017) Missing linkers: an alternative pathway to UiO-66 electronic structure engineering. Chem Mater 29:3006–3019. https://doi.org/10.1021/acs.chemmater.6b05444
43. Wen Y, Zhang P, Sharma VK et al (2021) Metal-organic frameworks for environmental applications. Cell Reports Phys Sci 2:100348. https://doi.org/10.1016/j.xcrp.2021.100348
44. Zhang Z, Li X, Liu B et al (2016) Hexagonal microspindle of NH2-MIL-101(Fe) metal-organic frameworks with visible-light-induced photocatalytic activity for the degradation of toluene. RSC Adv 6:4289–4295. https://doi.org/10.1039/c5ra23154j
45. Li X, Le Z, Chen X et al (2018) Graphene oxide enhanced amine-functionalized titanium metal organic framework for visible-light-driven photocatalytic oxidation of gaseous pollutants. Appl Catal B Environ 236:501–508. https://doi.org/10.1016/j.apcatb.2018.05.052
46. Kumar A (2017) A review on the factors affecting the photocatalytic degradation of hazardous materials. Mater Sci Eng Int J 1:106–114. https://doi.org/10.15406/mseij.2017.01.00018
47. Barka N, Qourzal S, Assabbane A et al (2008) Factors influencing the photocatalytic degradation of Rhodamine B by TiO_2-coated non-woven paper. J Photochem Photobiol A Chem 195:346–351. https://doi.org/10.1016/j.jphotochem.2007.10.022
48. Roy D, Neogi S, De S (2022) Visible light assisted activation of peroxymonosulfate by bimetallic MOF based heterojunction MIL-53(Fe/Co)/CeO_2 for atrazine degradation: pivotal roles of dual redox cycle for reactive species generation. Chem Eng J 430:133069. https://doi.org/10.1016/j.cej.2021.133069
49. Mosleh S, Rezaei K, Dashtian K, Salehi Z (2021) Ce/Eu redox couple functionalized HKUST-1 MOF insight to sono-photodegradation of malathion. J Hazard Mater 409:124478. https://doi.org/10.1016/j.jhazmat.2020.124478
50. Vaya D, Surolia PK (2020) Semiconductor based photocatalytic degradation of pesticides: an overview. Environ Technol Innov 20:101128. https://doi.org/10.1016/j.eti.2020.101128

51. Hayati P, Mehrabadi Z, Karimi M et al (2021) Photocatalytic activity of new nanostructures of an Ag(i) metal-organic framework (Ag-MOF) for the efficient degradation of MCPA and 2,4-D herbicides under sunlight irradiation. New J Chem 45:3408–3417. https://doi.org/10.1039/d0nj02460k
52. Xue Y, Wang P, Wang C, Ao Y (2018) Efficient degradation of atrazine by BiOBr/UiO-66 composite photocatalyst under visible light irradiation: environmental factors, mechanisms and degradation pathways. Chemosphere 203:497–505. https://doi.org/10.1016/j.chemosphere.2018.04.017
53. Nguyen VTT, Luu CL, Nguyen T et al (2020) Multifunctional Zn-MOF-74 as the gas adsorbent and photocatalyst. Adv Nat Sci Nanosci Nanotechnol 11. https://doi.org/10.1088/2043-6254/ab9d7c
54. Abdelhameed RM, Darwesh OM, El-Shahat M (2023) Titanium-based metal-organic framework capsulated with magnetic nanoparticles: antimicrobial and photocatalytic degradation of pesticides. Microporous Mesoporous Mater 354:112543. https://doi.org/10.1016/j.micromeso.2023.112543
55. Mon M, Bruno R, Ferrando-Soria J et al (2018) Metal-organic framework technologies for water remediation: towards a sustainable ecosystem. J Mater Chem A 6:4912–4947. https://doi.org/10.1039/c8ta00264a
56. Zhang X, Chen Z, Liu X et al (2020) A historical overview of the activation and porosity of metal-organic frameworks. Chem Soc Rev 49:7406–7427. https://doi.org/10.1039/d0cs00997k
57. Masoomi MY, Morsali A, Dhakshinamoorthy A, Garcia H (2019) Mixed-metal MOFs: unique opportunities in metal-organic framework (MOF) functionality and design. Angew Chemie 131:15330–15347. https://doi.org/10.1002/ange.201902229
58. Kalaj M, Cohen SM (2020) Postsynthetic modification: an enabling technology for the advancement of metal-organic frameworks. ACS Cent Sci 6:1046–1057. https://doi.org/10.1021/acscentsci.0c00690
59. Younis SA, Kwon EE, Qasim M et al (2020) Metal-organic framework as a photocatalyst: progress in modulation strategies and environmental/energy applications. Prog Energy Combust Sci 81:100870. https://doi.org/10.1016/j.pecs.2020.100870
60. Li J, Wang X, Zhao G et al (2018) Metal-organic framework-based materials: superior adsorbents for the capture of toxic and radioactive metal ions. Chem Soc Rev 47:2322–2356. https://doi.org/10.1039/c7cs00543a
61. Joseph L, Jun BM, Jang M et al (2019) Removal of contaminants of emerging concern by metal-organic framework nanoadsorbents: a review. Chem Eng J 369:928–946. https://doi.org/10.1016/j.cej.2019.03.173
62. Fakhri H, Bagheri H (2020) Highly efficient Zr-MOF@WO3/graphene oxide photocatalyst: synthesis, characterization and photodegradation of tetracycline and malathion. Mater Sci Semicond Process 107:104815. https://doi.org/10.1016/j.mssp.2019.104815
63. Oladipo AA, Vaziri R, Abureesh MA (2018) Highly robust $AgIO_3$/MIL-53 (Fe) nanohybrid composites for degradation of organophosphorus pesticides in single and binary systems: application of artificial neural networks modelling. J Taiwan Inst Chem Eng 83:133–142. https://doi.org/10.1016/j.jtice.2017.12.013
64. Ramezanalizadeh H, Manteghi F (2017) Immobilization of mixed cobalt/nickel metal-organic framework on a magnetic $BiFeO_3$: a highly efficient separable photocatalyst for degradation of water pollutions. J Photochem Photobiol A Chem 346:89–104. https://doi.org/10.1016/j.jphotochem.2017.05.041
65. Zhang Y, Liu S, Lu W et al (2011) In situ green synthesis of Au nanostructures on graphene oxide and their application for catalytic reduction of 4-nitrophenol. Catal Sci Technol 1:1142–1144. https://doi.org/10.1039/c1cy00205h
66. Samuel MS, Bhattacharya J, Parthiban C et al (2018) Ultrasound-assisted synthesis of metal organic framework for the photocatalytic reduction of 4-nitrophenol under direct sunlight. Ultrason Sonochem 49:215–221. https://doi.org/10.1016/j.ultsonch.2018.08.004

67. Liu J, Liu J, Xiong WH et al (2020) Developing a novel nanoscale porphyrinic metal-organic framework: a bifunctional platform with sensitive fluorescent detection and elimination of Nitenpyram in agricultural environment. J Agric Food Chem 68:5572–5578. https://doi.org/10.1021/acs.jafc.0c01313
68. Ahmad M, Chen S, Ye F et al (2019) Efficient photo-Fenton activity in mesoporous MIL-100(Fe) decorated with ZnO nanosphere for pollutants degradation. Appl Catal B Environ 245:428–438. https://doi.org/10.1016/j.apcatb.2018.12.057
69. Jonidi-Jafari A, Shirzad-Siboni M, Yang JK et al (2015) Photocatalytic degradation of diazinon with illuminated ZnO-TiO_2 composite. J Taiwan Inst Chem Eng 50:100–107. https://doi.org/10.1016/j.jtice.2014.12.020
70. Jonidi-Jafari A, Gholami M, Farzadkia M et al (2017) Application of Ni-doped ZnO nanorods for degradation of diazinon: kinetics and by-products. Sep Sci Technol 52:2395–2406. https://doi.org/10.1080/01496395.2017.1303508
71. Dong H, Zeng G, Tang L et al (2015) An overview on limitations of TiO_2-based particles for photocatalytic degradation of organic pollutants and the corresponding countermeasures. Water Res 79:128–146. https://doi.org/10.1016/j.watres.2015.04.038
72. Marschall R (2014) Semiconductor composites: Strategies for enhancing charge carrier separation to improve photocatalytic activity. Adv Funct Mater 24:2421–2440. https://doi.org/10.1002/adfm.201303214
73. Ibhadon AO, Fitzpatrick P (2013) Heterogeneous photocatalysis: recent advances and applications. Catalysts 3:189–218. https://doi.org/10.3390/catal3010189
74. Hlophe PV, Dlamini LN (2021) Photocatalytic degradation of diazinon with a 2d/3d nanocomposite of black phosphorous/metal organic framework. Catalysts 11. https://doi.org/10.3390/catal11060679
75. Sajjadi S, Khataee A, Bagheri N et al (2019) Degradation of diazinon pesticide using catalyzed persulfate with Fe_3O_4@MOF-2 nanocomposite under ultrasound irradiation. J Ind Eng Chem 77:280–290. https://doi.org/10.1016/j.jiec.2019.04.049
76. Geed SR, Kureel MK, Giri BS et al (2017) Performance evaluation of Malathion biodegradation in batch and continuous packed bed bioreactor (PBBR). Bioresour Technol 227:56–65. https://doi.org/10.1016/j.biortech.2016.12.020
77. Nasseri S, Omidvar Borna M, Esrafili A et al (2018) Photocatalytic degradation of malathion using Zn2+-doped TiO_2 nanoparticles: statistical analysis and optimization of operating parameters. Appl Phys A Mater Sci Process 124:1–11. https://doi.org/10.1007/s00339-018-1599-0
78. Kermani M, Mohammadi F, Kakavandi B et al (2018) Simultaneous catalytic degradation of 2,4-D and MCPA herbicides using sulfate radical-based heterogeneous oxidation over persulfate activated by natural hematite (α-Fe2O3/PS). J Phys Chem Solids 117:49–59. https://doi.org/10.1016/j.jpcs.2018.02.009
79. Del Ángel-Sanchez K, Vázquez-Cuchillo O, Aguilar-Elguezabal A et al (2013) Photocatalytic degradation of 2,4-dichlorophenoxyacetic acid under visible light: effect of synthesis route. Mater Chem Phys 139:423–430. https://doi.org/10.1016/j.matchemphys.2013.01.009
80. Ebrahimi R, Mohammadi M, Maleki A et al (2020) Photocatalytic degradation of 2,4-dichlorophenoxyacetic acid in aqueous solution using Mn-doped ZnO/graphene nanocomposite under LED radiation. J Inorg Organomet Polym Mater 30:923–934. https://doi.org/10.1007/s10904-019-01280-3
81. Li K, Wu JQ, Jiang LL et al (2017) Developmental toxicity of 2,4-dichlorophenoxyacetic acid in zebrafish embryos. Chemosphere 171:40–48. https://doi.org/10.1016/j.chemosphere.2016.12.032
82. Teklu BM, Adriaanse PI, Ter Horst MMS et al (2015) Surface water risk assessment of pesticides in Ethiopia. Sci Total Environ 508:566–574. https://doi.org/10.1016/j.scitotenv.2014.11.049
83. Pattappan D, Mohankumar A, Kumar RTR et al (2023) Visible light photocatalytic activity of a FeCo metal-organic framework for degradation of acetaminophen and 2,4-dichlorophenoxyacetic acid and a nematode-based ecological assessment. Chem Eng J 464:142676. https://doi.org/10.1016/j.cej.2023.142676

84. Feng S, Wang R, Feng S et al (2019) Synthesis of Zr-based MOF nanocomposites for efficient visible-light photocatalytic degradation of contaminants. Res Chem Intermed 45:1263–1279. https://doi.org/10.1007/s11164-018-3682-8
85. Balaji C, Moholkar VS, Pandit AB, Ashokkumar M (2011) Mechanistic investigations on sonophotocatalytic degradation of textile dyes with surface active solutes. Ind Eng Chem Res 50:11485–11494. https://doi.org/10.1021/ie201127v
86. Adewu-Yi YG (2005) Sonochemistry in environmental remediation. 2. Heterogeneous sonophotocatalytic oxidation processes for the treatment of pollutants in water. Environ Sci Technol 39:8557–8570. https://doi.org/10.1021/es0509127
87. Joseph CG, Li Puma G, Bono A, Krishnaiah D (2009) Sonophotocatalysis in advanced oxidation process: a short review. Ultrason Sonochem 16:583–589. https://doi.org/10.1016/j.ultsonch.2009.02.002
88. Sivakumar M, Tatake PA, Pandit AB (2002) Kinetics of p-nitrophenol degradation: effect of reaction conditions and cavitational parameters for a multiple frequency system. Chem Eng J 85:327–338. https://doi.org/10.1016/S1385-8947(01)00179-6
89. Yue X, Guo W, Li X et al (2016) Core-shell Fe3O4@MIL-101(Fe) composites as heterogeneous catalysts of persulfate activation for the removal of Acid Orange 7. Environ Sci Pollut Res 23:15218–15226. https://doi.org/10.1007/s11356-016-6702-5
90. Darvishi Cheshmeh Soltani R, Mashayekhi M (2018) Decomposition of ibuprofen in water via an electrochemical process with nano-sized carbon black-coated carbon cloth as oxygen-permeable cathode integrated with ultrasound. Chemosphere 194:471–480. https://doi.org/10.1016/j.chemosphere.2017.12.033
91. Mosleh S, Rahimi MR (2017) Intensification of abamectin pesticide degradation using the combination of ultrasonic cavitation and visible-light driven photocatalytic process: synergistic effect and optimization study. Ultrason Sonochem 35:449–457. https://doi.org/10.1016/j.ultsonch.2016.10.025
92. Zhang H, Qiao J, Li G et al (2018) Preparation of Ce4+-doped BaZrO3 by hydrothermal method and application in dual-frequent sonocatalytic degradation of norfloxacin in aqueous solution. Ultrason Sonochem 42:356–367. https://doi.org/10.1016/j.ultsonch.2017.11.043
93. Jorfi S, Pourfadakari S, Kakavandi B (2018) A new approach in sono-photocatalytic degradation of recalcitrant textile wastewater using MgO@Zeolite nanostructure under UVA irradiation. Chem Eng J 343:95–107. https://doi.org/10.1016/j.cej.2018.02.067
94. Kim DK, He Y, Jeon J, O'Shea KE (2016) Irradiation of ultrasound to 5-methylbenzotriazole in aqueous phase: degradation kinetics and mechanisms. Ultrason Sonochem 31:227–236. https://doi.org/10.1016/j.ultsonch.2016.01.006
95. Debabrata P, Sivakumar M (2018) Sonochemical degradation of endocrine-disrupting organochlorine pesticide Dicofol: investigations on the transformation pathways of dechlorination and the influencing operating parameters. Chemosphere 204:101–108. https://doi.org/10.1016/j.chemosphere.2018.04.014
96. Shi C, Qin L, Wu S et al (2021) Highly sensitive SERS detection and photocatalytic degradation of 4-aminothiophenol by a cost-effective cobalt metal–organic framework-based sandwich-like sheet. Chem Eng J 422:129970. https://doi.org/10.1016/j.cej.2021.129970
97. Gong J, Zhang W, Sen T et al (2021) Metal-organic framework MIL-101(Fe) nanoparticles decorated with Ag nanoparticles for regulating the photocatalytic phenol oxidation pathway for Cr(VI) reduction. ACS Appl Nano Mater 4:4513–4521. https://doi.org/10.1021/acsanm.1c00119
98. Khodkar A, Khezri SM, Pendashteh A et al (2018) Preparation and application of α-Fe2O3@MIL-101(Cr)@TiO2 based on metal–organic framework for photocatalytic degradation of paraquat. Toxicol Ind Health 34:842–859. https://doi.org/10.1177/0748233718797247
99. Duan X, Ao Z, Li D et al (2016) Surface-tailored nanodiamonds as excellent metal-free catalysts for organic oxidation. Carbon N Y 103:404–411. https://doi.org/10.1016/j.carbon.2016.03.034

100. Heu R, Ateia M, Yoshimura C et al (2020) Photocatalytic degradation of organic micropollutants in water by zr-mof/go composites. J Compos Sci 4:1–21. https://doi.org/10.3390/jcs4020054
101. Devarayapalli KC, Vattikuti SVP, Sreekanth TVM et al (2020) Hydrogen production and photocatalytic activity of g-C3N4/Co-MOF (ZIF-67) nanocomposite under visible light irradiation. Appl Organomet Chem 34:1–9. https://doi.org/10.1002/aoc.5376
102. Vattikuti SVP, Police AKR, Shim J, Byon C (2018) In situ fabrication of the Bi_2O_3–V_2O_5 hybrid embedded with graphitic carbon nitride nanosheets: oxygen vacancies mediated enhanced visible-light–driven photocatalytic degradation of organic pollutants and hydrogen evolution. Appl Surf Sci 447:740–756. https://doi.org/10.1016/j.apsusc.2018.04.040